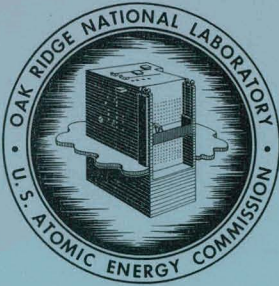


6-12-67

OK  
T

MASTER



# OAK RIDGE NATIONAL LABORATORY

operated by

UNION CARBIDE CORPORATION

NUCLEAR DIVISION

for the

U.S. ATOMIC ENERGY COMMISSION



ORNL - TM - 1789

76

## A SURVEY OF EQUILIBRIUM FUEL-CYCLE COSTS FOR A LOW-ENRICHED, UNCLAD, HELIUM-COOLED UO<sub>2</sub>-GRAPHITE REACTOR

He

C. M. Podeweltz

**NOTICE** This document contains information of a preliminary nature and was prepared primarily for internal use at the Oak Ridge National Laboratory. It is subject to revision or correction and therefore does not represent a final report.

THIS DOCUMENT HAS BEEN REVIEWED,  
NO INVENTIONS OR PATENT INTEREST  
TO THE A.E.C. AND DISCLOSED THEREIN.

B  
6/12/67

DISTRIBUTION OF THIS DOCUMENT IS UNLIMITED

leg

## **DISCLAIMER**

**This report was prepared as an account of work sponsored by an agency of the United States Government. Neither the United States Government nor any agency Thereof, nor any of their employees, makes any warranty, express or implied, or assumes any legal liability or responsibility for the accuracy, completeness, or usefulness of any information, apparatus, product, or process disclosed, or represents that its use would not infringe privately owned rights. Reference herein to any specific commercial product, process, or service by trade name, trademark, manufacturer, or otherwise does not necessarily constitute or imply its endorsement, recommendation, or favoring by the United States Government or any agency thereof. The views and opinions of authors expressed herein do not necessarily state or reflect those of the United States Government or any agency thereof.**

## **DISCLAIMER**

**Portions of this document may be illegible in electronic image products. Images are produced from the best available original document.**

#### LEGAL NOTICE

This report was prepared as an account of Government sponsored work. Neither the United States, nor the Commission, nor any person acting on behalf of the Commission:

- A. Makes any warranty or representation, expressed or implied, with respect to the accuracy, completeness, or usefulness of the information contained in this report, or that the use of any information, apparatus, method, or process disclosed in this report may not infringe privately owned rights; or
- B. Assumes any liabilities with respect to the use of, or for damages resulting from the use of any information, apparatus, method, or process disclosed in this report.

As used in the above, "person acting on behalf of the Commission" includes any employee or contractor of the Commission, or employee of such contractor, to the extent that such employee or contractor of the Commission, or employee of such contractor prepares, disseminates, or provides access to, any information pursuant to his employment or contract with the Commission, or his employment with such contractor.

ORNL-TM-1789

CFSTI PRICES

Contract No. W-7405-eng-26

H.C. \$ 3.00 MN .65

Reactor Division

A SURVEY OF EQUILIBRIUM FUEL-CYCLE COSTS FOR A LOW-ENRICHED,  
UNCLAD, HELIUM-COOLED  $UO_2$ -GRAPHITE REACTOR

C. M. Podeweltz

JUNE 1967

**LEGAL NOTICE**

This report was prepared as an account of Government sponsored work. Neither the United States, nor the Commission, nor any person acting on behalf of the Commission:

A. Makes any warranty or representation, expressed or implied, with respect to the accuracy, completeness, or usefulness of the information contained in this report, or that the use of any information, apparatus, method, or process disclosed in this report may not infringe privately owned rights; or

B. Assumes any liabilities with respect to the use of, or for damages resulting from the use of any information, apparatus, method, or process disclosed in this report.

As used in the above, "person acting on behalf of the Commission" includes any employee or contractor of the Commission, or employee of such contractor, to the extent that such employee or contractor of the Commission, or employee of such contractor prepares, disseminates, or provides access to, any information pursuant to his employment or contract with the Commission, or his employment with such contractor.

OAK RIDGE NATIONAL LABORATORY  
Oak Ridge, Tennessee  
operated by  
UNION CARBIDE CORPORATION  
for the  
U. S. ATOMIC ENERGY COMMISSION

DISTRIBUTION OF THIS DOCUMENT IS UNLIMITED

THIS PAGE  
WAS INTENTIONALLY  
LEFT BLANK

## CONTENTS

	<u>Page</u>
SUMMARY .....	v
ABSTRACT .....	1
I. INTRODUCTION .....	1
1. Objectives .....	1
2. The Fuel Element and the Reactor .....	2
II. PHYSICS .....	4
1. General .....	4
2. Resonance Absorption and the Dancoff Corrections ...	5
3. The Fast Fission Effect .....	6
4. Reactivity and Depletion Calculations .....	8
III. ECONOMICS .....	10
1. General .....	10
2. Bases for Cost Estimates .....	13
Inventory Fixed Charges .....	13
Burnup .....	13
Fabrication Unit Costs .....	13
Shipping Unit Costs .....	15
Reprocessing Unit Costs .....	15
Storage Unit Costs .....	15
Interest on Working Capital .....	15
3. Results .....	16
Conversion Ratios and Burnup .....	16
Fuel-Cycle Costs .....	20
IV. CONCLUSIONS .....	25
ACKNOWLEDGMENTS .....	27
REFERENCES .....	29
APPENDIX A: Determination of the Dancoff Factor .....	31
1. Application of Experimental Data .....	31
2. Theoretical Calculations .....	32
APPENDIX B: Heterogeneity of the Fast Effect .....	36

## CONTENTS (contd)

	<u>Page</u>
APPENDIX C: Tables of Results .....	41
1. Conversion Ratio and Burnup .....	41
2. Specific Power, Throughput and Component Fuel- Cycle Costs .....	42

## SUMMARY

A survey of equilibrium, fuel-cycle costs, associated with various combinations of lattice pitches, enrichments, and fuel-hole sizes, has been carried out for a gas-cooled, unclad,  $\text{UO}_2$ -graphite reactor. The  $\text{UO}_2$  was assumed to be formed into pellets, with no coating applied. The values of enrichment examined were: natural, 1, 2, 3, and 5%; of lattice pitch: 9, 10.8, 13.0, and 14.8 in.; and of fuel-hole diameter: 0.375 and 0.576 in. Nineteen  $\text{UO}_2$  holes and 42 coolant channels of 0.576-in. diameter were assumed to be drilled into a solid, hexagonal, graphite log. Holes and channels formed a central cluster, arranged on an equilateral-triangle spacing of 0.63 in.

Multigroup physics calculations were performed. The GAM-1 and GAM-2 codes were used to calculate resonance-region, self-shielded cross sections, and the THERMOS code was used to calculate weighted thermal cross sections. An auxiliary investigation into the best method of calculating Dancoff factors — best in the sense of producing GAM-2 calculated resonance-escape probabilities for  $^{238}\text{U}$  in agreement with Hellstrand's measurements on  $\text{UO}_2$  clusters — revealed the theoretical tables (ANL-5800) of the Dancoff-Ginsburg factor to be most suitable. A method based on analogous, fast-group Dancoff factors was devised to estimate the effect of heterogeneity on the fast-fission factor.

Depletion calculations utilizing the GAM-THERMOS cross sections were made with a multigroup, zero-dimensional computer code. Bucklings were supplied commensurate with the reactor sizes required to produce 1900 Mw (thermal) and, under the assumption of 40% efficiency, 760 Mw(e). A maximum  $\text{UO}_2$  temperature of 3032°F, coolant inlet and outlet temperatures of 720°F and 1470°F respectively, a core height of 25 ft and a pressure drop of 16.83 psia were specified thermodynamic parameters, which fixed the power in the maximum-power-producing cell (fuel element) at 2.586 Mw. Average power densities for the various cell sizes ranged from 5.35 to 1.98 w/cm<sup>3</sup>.

Economics calculations were made assuming equilibrium-cycle, graded-exposure conditions. Only non-recycle modes were considered. Fixed

charges on fuel inventories and fabrication plant working capital were 10%. Depreciating capital fixed charges on the fabrication and reprocessing plants were 22%. A plutonium credit of \$10/g fissile was allowed. Prices of uranium feed were taken from the current AEC cost schedule. A single-purpose reprocessing plant and a single-purpose fabrication plant, each of 15,000 Mw(e) capacity, were assumed to be located at the same site. An average reactor plant factor of 0.8 was assumed.

Two sets of fabrication unit costs were estimated, using HTGR fuel element data as a basis for extrapolation. One set was for cells (fuel elements) with small fuel holes, the other for cells with large fuel holes. The difference between the two was considerable, primarily because a fuel element with large fuel holes has a linear density of  $UO_2$  more than twice that of a fuel element with small fuel holes.

Fuel-cycle costs were computed for the situation where the spent fuel is reprocessed and sold, and for the situation where the fuel is "thrown away," or stored. The minimum "throwaway cycle" cost was found to be essentially the same as the minimum cost with fuel reprocessing for the large-fuel-hole reactors [1.163 as compared to 1.160 mills/kwhr(e)], and slightly lower for the small-fuel-hole reactors [1.314 vs 1.348 mills/kwhr(c)]. Minimum fuel-cycle costs were obtained in the 2-3% enrichment range for the small-fuel-hole reactors and in the 1.5-2.0% range for the large-fuel-hole reactors. The lower unit fabrication cost of the large-fuel-hole reactors was principally responsible for their lower, minimum total fuel-cycle costs.

For the set of small-fuel-hole reactors a minimum (throwaway) fuel-cycle cost of 1.314 mills/kwhr(e) was found. Associated with this minimum was a conversion ratio of 0.551 and a burnup of 41,083 Mwd/T. For the set of large-fuel-hole reactors a lowest, but not necessarily minimum, (reprocessed) cost of 1.160 mills/kwhr(e) was found.\* Its associated

---

\* Only the 13.0-in. and 14.8-in. lattice pitches were investigated for the large-fuel-hole reactors. Fuel-cycle costs were still found to be decreasing with increasing lattice pitch at 14.8 in.; whereas fuel-cycle costs for the small-fuel-hole reactors passed through a minimum in the broad range of 11 to 13 in.

conversion ratio and burnup were 0.637 and 29,400 Mwd/T, respectively. The largest conversion ratio reached in the study was 0.724 and was obtained for a large-fuel-hole reactor of 1% enrichment. Its associated fuel-cycle cost was 1.292 mills/kwhr(e).

# A SURVEY OF EQUILIBRIUM FUEL-CYCLE COSTS FOR A LOW-ENRICHED, UNCLAD, HELIUM-COOLED $\text{UO}_2$ -GRAPHITE REACTOR

C. M. Podeweltz

## ABSTRACT

A survey of equilibrium, fuel-cycle costs associated with various combinations of lattice pitch, enrichment and fuel-hole size has been carried out for a gas-cooled, unclad,  $\text{UO}_2$ -graphite reactor. The  $\text{UO}_2$  was assumed to be formed into pellets with no coating applied. Nineteen  $\text{UO}_2$  holes intermingled with 42 coolant channels comprised a central cluster region in the graphite cell. Enrichment was varied in the range of natural to 5%; lattice pitch in the range of 10.8 to 14.8 in. Two fuel-hole diameters, 0.375 and 0.576 in., were investigated. The reactor was assumed to deliver 1900 Mw(thermal) and 760 Mw(e).

Multigroup, point-depletion calculations of the homogenized cell were performed utilizing GAM self-shielded, resonance cross sections and flux-weighted THERMOS cross sections. For the set of small fuel-hole reactors a minimum fuel-cycle cost of 1.314 mills/kwhr(e) was found. The reactor for which this cost obtained had a conversion ratio of 0.551, and a burnup of 41,083 Mwd/T. For the large fuel-hole set the corresponding values were 1.160, 0.637, and 29,400.

---

## I. INTRODUCTION

### 1. Objectives

The study which is described herein was undertaken to determine whether a gas-cooled, unclad, uranium-graphite reactor of heterogeneous structure might offer fuel-cycle cost advantages over a homogeneous, or semihomogeneous reactor of similar material composition.

A primary cost advantage would be expected to arise from the utilization of less highly enriched fuel. On the other hand a heterogeneous lattice would require a larger inventory of uranium. This increased inventory would tend to offset decreased enrichment. Adding to these

conflicting factors are the possibly considerable differences in the unit costs for fabricating and processing the two types of fuels.

Finally — although fuel-cycle costs are the primary object of attention in this study — it should be borne in mind that capital costs for the heterogeneous reactors would usually be higher due to their generally lower power densities.

## 2. The Fuel Element and the Reactor

The basic cell investigated in this study was a cluster of 19  $\text{UO}_2$ -filled holes intermingled with 42 (helium) coolant channels, all centralized in a hexagonal graphite log of varying dimensions. The cluster dimension (across the flats) was held invariant at  $\sim 5$  in. The coolant channels were fixed at 0.576 in. in diameter and were spaced 0.630-in. apart, forming hexagons around each fuel hole. The  $\text{UO}_2$  holes were arranged on an equilateral-triangle pitch of 1.091 in. Graphite occupied the remaining space within the cluster. The cell, which was also taken as the reactor fuel element in the economics calculations, is shown in Fig. 1.

Three parameters, fuel-hole diameter, fuel enrichment, and cell lattice pitch, were varied and their various combinations studied. The first fuel-hole diameter was chosen as 0.375 in. Enrichment was varied through the values natural, 1, 2, 3, and 5%; and lattice pitch (or cell dimension across the flats) through the values 9, 10.8, 13.0, and 14.8 in. The effect of increasing the fuel-hole diameter to 0.576 in. was subsequently studied over the same range of enrichments. The values of lattice pitch, however, were limited, because of time considerations, to 13.0 and 14.8 in.

The reactor core was assumed to consist of approximately 1027 cells, producing a combined total power of 1900 Mw(thermal) and 760 Mw(e). Power in the central cell was limited to 2.586 Mw from temperature considerations, and a radial peak-to-average power value of 1.4 was assumed. The core length was fixed at 25 ft. A graphite reflector of effectively infinite thickness was assumed to surround the core.

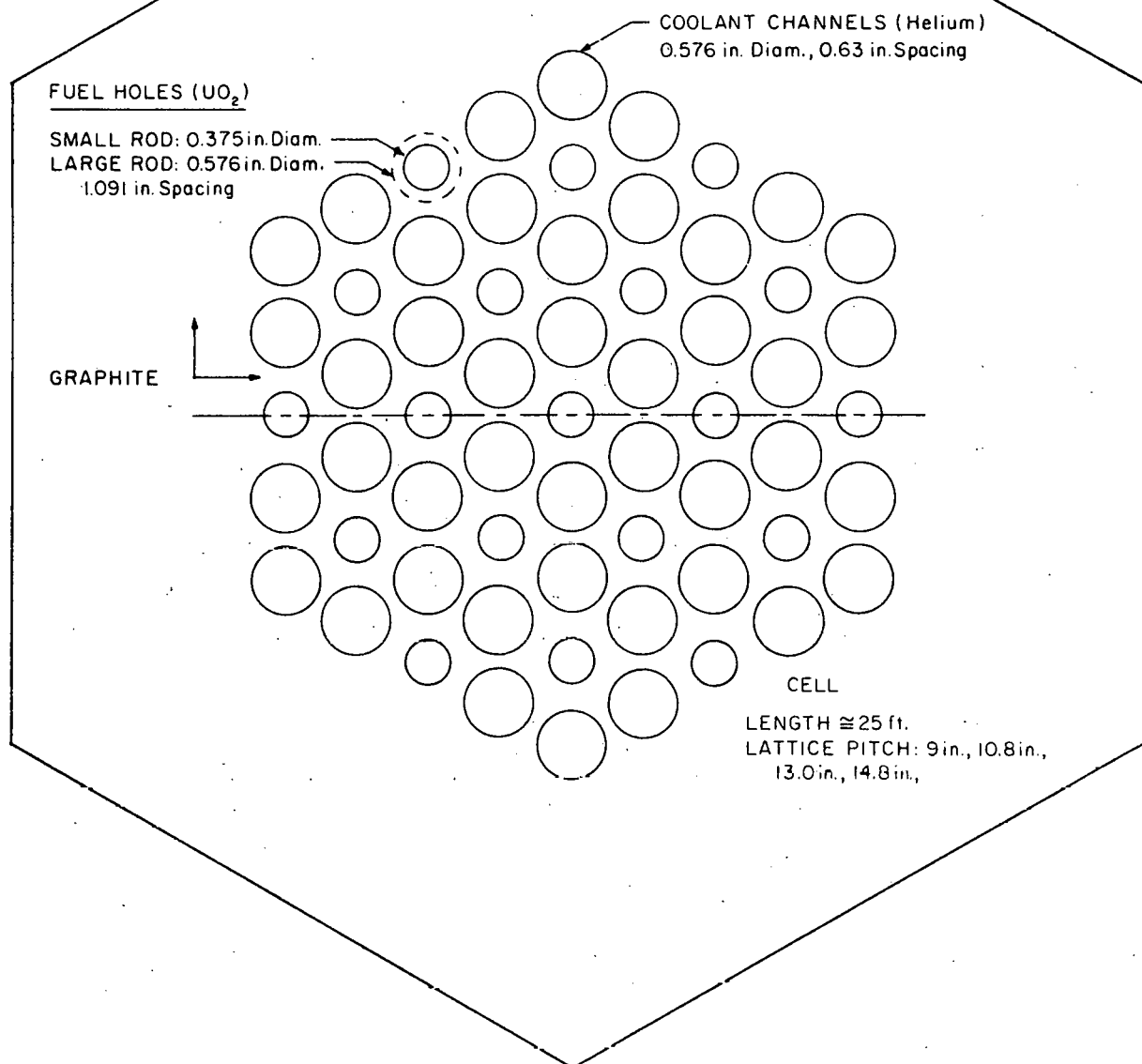


Fig. 1. Unit Cell (Fuel Element).

## II. PHYSICS

### 1. General

The final steps in the physics portion of the analysis are multi-group, point-depletion calculations programmed for the IBM 7090 computer.<sup>1</sup> These computations of multiplication factors and time-varying nuclide concentrations assume fuel and moderator are homogeneously mixed. Because this assumption is inherent in the calculation, the effects of cell heterogeneity must be introduced with the input in the form of self-shielded cross section data.

The preparation of such data has entailed the use of methods which in detail analyze the aspects of neutron behavior generally grouped, for low-enriched fuel, under the convenient headings of fast fission, resonance absorption and thermal utilization. In the latter two areas the methods utilized were the GAM codes<sup>2,3</sup> and the THERMOS code<sup>4</sup> respectively; while for fast fission, since no code was available, a one-group method was devised for hand analysis of the heterogeneity effect.

In the case of thermal utilization - which for the purpose of correlation with THERMOS calculations may be taken as covering the range 0.005 to 0.876 ev - the cluster was homogenized into a single inner cylindrical region, with an outer region of pure graphite. The geometry, along with the appropriate nuclide densities (including fission and capture products and reduced uranium densities representative of the equilibrium condition) were fed to the THERMOS code. The code then calculated weighted, microscopic cross sections of the elements based on the flux distributions over the outer and inner regions. Flux depressions within the individual fuel elements, the so-called "fine structure," were neglected.

On the other hand, a knowledge of neutron absorption within an individual fuel hole is essential to the evaluation of the effects of heterogeneous geometry upon the group-averaged, microscopic cross sections of the resonance nuclides. But to gain this knowledge requires the solution of a corollary problem concerning the effects of nearby fuel holes on the resonance-energy fluxes at the surface of the fuel hole under consideration. This problem is not solved by GAM-1 or GAM-2, and it is left to the code

user to supply the appropriate resonance-region Dancoff factor which accounts for interaction with nearby fuel holes.

The solution to the problem of heterogeneous fast fission, as presented in this report, similarly depends upon the estimation of a Dancoff factor for the energy region above  $^{238}\text{U}$  fission threshold.

The requirement for fairly accurate Dancoff factors, especially in the case of resonance absorption calculations, prompted an auxiliary investigation into the best method of estimating such factors. The criterion for the "best method" was that it should give Dancoff factors which, when used in GAM-2,  $^{238}\text{U}$ , resonance-absorption computations, would yield resonance-escape probabilities that were in good agreement with those inferred from Hellstrand's measurements on  $\text{UO}_2$  rods in cluster geometry.<sup>5</sup>

The following paragraphs will briefly discuss the results of the investigations into Dancoff factors and fast effect and will conclude with a section on the point-depletion calculations. The thermal calculations need not be taken up further since a straightforward application of the THERMOS code to the approximate cell geometry mentioned above produced the thermal-region cross sections required for the point-depletion calculations.

## 2. Resonance Absorption and the Dancoff Corrections

The calculations which were done to determine the best Dancoff factor formed two parts. In the first, the experimental data of Hellstrand<sup>5</sup> was used to establish the effective resonance integral of  $^{238}\text{U}$  in  $\text{UO}_2$  cluster geometry. The resonance-escape probability based on this integral then provided the norm against which the theoretical GAM-2 calculations, comprising the second part of the calculations, could be compared.

The details of the calculations and the considerations entering into the comparison are given in Appendix A. In effect, alternate methods of hand calculating the Dancoff factor were tried: the rational approximation, Sauer's approximation,<sup>6</sup> and the Dancoff-Ginsburg tables of ANL-5800.<sup>7</sup> Each factor thus obtained was entered into a GAM-2 calculation, and the associated resonance-escape probability of  $^{238}\text{U}$  was computed from the output group cross sections.

The method which produced the best agreement with the resonance-escape probability based on the Hellstrand data was the one which utilized the ANL-5800 tables. The results of the calculations are exhibited in Tables 1 and 2. In Table 1  $(S_{\text{eff}}/M)_{\text{UO}_2}$  denotes the effective surface-to-mass ratio of the  $\text{UO}_2$  cluster.

Table 1. Resonance Integrals and Escape Probabilities for  $^{238}\text{U}$ , Utilizing Hellstrand's Experimental Data for  $\text{UO}_2$  Cluster

Lattice	$(S_{\text{eff}}/M)_{\text{UO}_2}$ ( $\text{cm}^2/\text{g}$ )	Resonance- Integral <sup>a</sup> (barns)	Atom Ratio: $N_{\text{C}}/N_{28}$ (in cell)	Resonance- Escape Probability <sup>b</sup>
Small fuel-hole, 9-in.	0.333	20.940	97.19	0.751
Large fuel-hole, 13-in.	0.151	15.867	93.35	0.799

<sup>a</sup>Computed from Eq. (A.2) of Appendix A.

<sup>b</sup>Computed from Eq. (A.3) of Appendix A.

### 3. The Fast Fission Effect

The fast effect is implicit in, but not explicitly determined by, the point, multigroup calculation of  $k_{\text{eff}}$ . When the fuel and moderator are assumed homogeneously mixed, the fast effect is not given its proper weight. This is because homogenization changes the neutron's probability of colliding with fuel atoms before being degraded below fission threshold.

As in the cases of resonance and thermal reactions, it is possible to rectify the situation by inputting "advantaged" parameters in order to force the code to account correctly for the heterogeneity of the cell. The manner in which this was done is described in Appendix B.

The substance of the procedure is to calculate homogeneous and heterogeneous fast-fission factors ( $\epsilon$ ) for the same cell by following the successive collisions in the fast sub-cycle. Knowing these one can then alter one or more parameters — in this study  $\nu$ , the number of neutrons born per  $^{238}\text{U}$  fission — in such a way as to transform the homogeneous  $\epsilon$

Table 2. GAM-2 Resonance-Escape Probabilities vs Dancoff Factor

Method or Approximation for Computing Dancoff Factor	Value of Dancoff Factor, C	GAM-2 Resonance- Escape Probability for $^{238}\text{U}$
A. Small Fuel-Hole Cluster, 9-in. Lattice		
Isolated rod	0	0.731
Rational, infinite array ( $C_R$ )	0.427	0.780
Rational, finite cluster ( $\bar{C}_R$ )	0.311 <sup>a</sup>	0.767 <sup>b</sup>
Sauer, infinite array ( $C_S$ )	0.393	0.776
Sauer, finite cluster ( $\bar{C}_S$ )	0.285 <sup>a</sup>	0.764 <sup>b</sup>
ANL-5800 tables, infinite array ( $C_D$ )	0.286	0.764
ANL-5800 tables, finite cluster ( $\bar{C}_D$ )	0.195	0.753
Experimental, Hellstrand cluster data	0.175 <sup>c</sup>	
B. Large Fuel-Hole Cluster, 13-in. Lattice		
Isolated rod	0	0.761
Dancoff tables, finite cluster ( $\bar{C}_D$ )	0.384	0.797
Experimental, Hellstrand cluster data	0.400 <sup>c</sup>	

<sup>a</sup>Dancoff factor interpolated, based on corresponding resonance-escape probabilities.

<sup>b</sup>Computed from Eq. (A.8) of Appendix A.

<sup>c</sup>Dancoff factor inferred, based on experimental value of resonance-escape probability given in Table 1.

into a heterogeneous  $\epsilon$ . It is shown in Appendix B that an alteration of parameters based on this criterion will then inject a correction for fast-fission heterogeneity into the multigroup calculation, which is quite accurate for  $k_{\text{eff}}$  values near one.

Table 3 summarizes the homogeneous and heterogeneous  $\epsilon$ 's calculated for the different lattices. Also given is the altered  $\nu$  value,  $\nu'$ , which, when substituted into the expression for  $\epsilon_{\text{hom}}$  (Eq. B.2 of Appendix B), produces the same value as that computed from the expression for  $\epsilon_{\text{het}}$  (Eq. B.1) using the correct  $\nu$  value.  $V^m/V^f$  is the volume ratio of carbon to  $\text{UO}_2$ ;  $C$  is the fast-group Dancoff factor;  $P_c^f$  is the Dancoff-corrected, first-flight, fuel collision probability;  $\epsilon_{\text{hom}}$  and  $\epsilon_{\text{het}}$  are the homogeneous and heterogeneous fast fission factors.

Table 3. Heterogeneous and Homogeneous Fast Fission Factors

Lattice Pitch (in.)	$V^m/V^f$	$C^a$	$P_c^f$	$\epsilon_{\text{hom}}$	$\epsilon_{\text{het}}$	$\nu'$
Small fuel-hole						
9.0	27.236	0.280	0.203	1.0117	1.0182	3.609
10.8	42.082	0.280	0.203	1.0078	1.0154	4.288
13.0	63.119	0.280	0.203	1.0053	1.0136	5.246
14.8	84.199	0.280	0.203	1.0040	1.0126	6.176
Large fuel-hole						
13.0	26.175	0.447	0.355	1.0122	1.0275	4.753
14.8	35.103	0.447	0.355	1.0092	1.0257	5.527

<sup>a</sup>The interaction between clusters was neglected, hence  $C$  and  $P_c^f$  remain constant for a given cluster geometry.

#### 4. Reactivity and Depletion Calculations

The LTM computer code<sup>1</sup> calculates the time-dependent concentrations of fission-product and heavy-element nuclides on the basis of spatially independent equations, and for a specified average reactor power density. The finiteness of the system, and therefore the leakage, is carried in the

DB<sup>2</sup> term supplied for each energy group as input. The relation of the B<sup>2</sup> value to the total power requirements will be discussed in the economics section. In the small-fuel-hole lattices leakage accounted for 1% to 1.5% of the total neutron losses. In the large-fuel-hole lattices losses of 1.5% to 2.5% were seen.

Equilibrium-cycle and graded-exposure conditions were assumed to prevail. The fuel-residence time was determined as that time up to which the time integral of the neutron productions equals the time integral of the neutron losses (i.e.,  $\bar{k}_{\text{eff}} = 1$ ; no control poisons were assumed to be present in this study). The flux spectrum in LTM is not varied with time but is computed from nuclide densities time-averaged over the fuel life-time and maintained constant for a given fuel-cycle calculation. Since the flux spectrum in turn determines the average nuclide densities, the calculation is iterative. Fuel-residence times are recalculated until the average nuclide densities over the last iteration cycle agree, within a specified tolerance, with those from the next-to-last iteration cycle.

The treatment of fission-product nuclide chains conformed in general to the "short fission-product treatment" described in Part II of the advanced converter study.<sup>8</sup> The use of two pseudoelements as non-saturating and slowly saturating lumped fission products reduces the large number of nuclide chains which are actually present to the most important chains. <sup>135</sup>Xe, <sup>146</sup>Nd, <sup>147</sup>Pm, <sup>148</sup>Pm, <sup>149</sup>Sm, <sup>150</sup>Sm, <sup>151</sup>Sm, and <sup>152</sup>Sm were treated explicitly. The treatment of heavy-element buildup was terminated at <sup>237</sup>Np in the <sup>235</sup>U chain, and at <sup>242</sup>Pu, omitting <sup>239</sup>Np, in the <sup>238</sup>U chain.

Since recycle of fuel was not considered in this study, the initial fuel was fresh UO<sub>2</sub>, in the proportion and enrichment characteristic of the particular lattice under consideration. An option in LTM permitting the printout of the  $k_{\text{eff}}$  value at the initiation of the cycle was therefore exercised to obtain the clean, effective-multiplication factor of the lattice. These are listed in Table 4. None of the natural uranium lattices were critical at equilibrium conditions. The 1% enriched 9-in., small-fuel-hole lattice was also subcritical.

Table 4. Clean, Effective-Multiplication Factors of  
Unclad,  $\text{UO}_2$ -Graphite Lattices

Pitch <sup>a</sup> (in.)	Enrichment (%)				
	Natural	1	2	3	5
9.0 (S) <sup>b</sup>	Not critical <sup>d</sup>	Not critical	1.120	1.284	1.356
10.8 (S)	Not critical	1.068	1.301	1.399	1.483
13.0 (S)	Not critical	1.092	1.352	1.466	1.567
14.8 (S)	Not critical	1.083	1.363	1.488	1.604
13.0 (L) <sup>c</sup>	Not critical	1.068	1.285	1.371	1.446
14.8 (L)	Not critical	1.101	1.339	1.438	1.520

<sup>a</sup>Center-to-center distance between clusters, which are composed of 19  $\text{UO}_2$  holes, spaced 1.091 in. apart, intermingled with 42 helium coolant channels of 0.288 in. radius, spaced 0.63 in. apart. The remaining volume is graphite.

<sup>b</sup>(S) denotes small-fuel-hole lattice; radius of hole = 0.1875 in.

<sup>c</sup>(L) denotes large-fuel-hole lattice; radius of hole = 0.288 in.

<sup>d</sup>"Not critical" implies not critical in equilibrium condition.

### III. ECONOMICS

#### 1. General

Fuel-cycle costs associated with the different combinations of lattice pitch, enrichment, and fuel-hole size were computed by the economics portion of the LTM computer code. As mentioned in the previous section graded-exposure and equilibrium cycle conditions were assumed. The spent fuel was either considered to be reprocessed and sold, or "thrown away," i.e., stored, upon discharge; costs were computed in each case. Recycle of fuel was not considered, primarily because the results obtained from a previous study of a homogeneous, carbon-uranium, coated-particle system<sup>9</sup> showed non-recycle to be less costly for low-enriched uranium fuels.

The general ground rules for the fuel-cycle analysis of this study were chosen from among the options considered in the advanced-converter study.<sup>8</sup> Thus, the size of the reactor industry was assumed to be 15,000

Mw of electrical power, serviced by a single-purpose, privately-owned fabrication plant and a single-purpose, privately-owned reprocessing plant. Both are located at the same site and utilize privately-owned fuel. However the bases for estimating the unit costs of fuel fabrication, reprocessing, and shipping need more specific discussion since they cannot be inferred directly from data presented in the advanced converter study. A full resume' of the financial ground rules therefore is deferred until the next section. A list of the fixed parameters assumed in the study, excluding fabrication, reprocessing, and shipping unit costs, is given in Table 5.

The average power density supplied to LTM for a particular block size was based on an allowable power output of 2.586 Mw for the maximum power producing cell. A heat-transfer study based on the small-fuel-hole, 9-in. lattice cell established this criterion.<sup>10</sup> Other parameters assumed were a core height of 25 ft, an inlet temperature of 720°F, an outlet temperature of 1470°F, and a pressure drop of 16.83 psia. The maximum fuel temperature was limited to 3032°F, implying a maximum average power density for the 9-in. cell of 5.35 w/cm<sup>3</sup> and a total power output of 2.586 Mw. Average power densities for the other size cells were obtained holding this latter number constant. A change in fuel-hole size required no further compensating changes in cell power density, since temperature conditions do not change significantly if the coolant-channel parameters and power output per unit length of fuel remain the same.\*

The geometric bucklings supplied to LTM implied reactor sizes requisite to a total core power output of ~1900 Mw (thermal), assuming a radial peak-to-average power density ratio of 1.4. Eighteen hexagonal rings of cells, or 1027 cells, would therefore be required, causing the core diameter to range from 27 ft for the 9-in. lattice to 44 ft for the 14.8-in. lattice. An overall thermal efficiency of 0.4 was assumed, thus fixing gross electrical power output at 760 Mw.

---

\* Actually a decrease in graphite thickness between fuel hole and coolant channel will cause a small drop in the average graphite and fuel temperatures.

Table 5. Fixed Parameters Assumed in Economics Calculations

---

Thermal efficiency, %	40
Maximum fuel temperature, °F	3032
Inlet coolant temperature, °F	720
Outlet coolant temperature, °F	1470
Pressure drop, psi	16.83
Number of coolant channels	42
Diameter of coolant channels, in.	0.576
Distance between adjacent coolant channels, in.	0.63
Number of fuel holes per cluster	19
Diameter of fuel hole, in.	
Small rod	0.375
Large rod	0.576
Fuel hole spacing, in.	1.091
Cluster-region area, in. <sup>2</sup>	21.11
Power density, w/cm <sup>3</sup>	
9.0-in. lattice pitch	5.36
10.8-in. lattice pitch	3.71
13.0-in. lattice pitch	2.58
14.8-in. lattice pitch	1.98
Buckling, cm <sup>-2</sup>	
9.0-in. lattice pitch	$4.0 \times 10^{-5}$
10.8-in. lattice pitch	$3.3 \times 10^{-5}$
13.0-in. lattice pitch	$2.7 \times 10^{-5}$
14.8-in. lattice pitch	$2.4 \times 10^{-5}$
Fixed charges on inventory, %	10
Fabrication and reprocessing plant amortization, %	22
Reactor plant lifetime, years	30
Reactor plant factor	0.8
Fabrication holdup time, days	150
Processing holdup time, days	150
Size of reactor industry, Mw(e)	15,000
Processing losses, %	1.0
Fabrication scrap losses, %	0.2
Unit feed cost, \$/g of fissile material	Current AEC cost schedule
Plutonium price, \$/g fissile	10.00

---

## 2. Bases for Cost Estimates

Inventory Fixed Charges. Private ownership of fuel and of fabrication and reprocessing plants was assumed. Inventory charges for fissile material, whether in core or in the fabrication and reprocessing inventories, were fixed at 10% per year. Core inventory charges were computed on the worth of the equilibrium, total fissile inventory in the core. Fabrication and reprocessing inventory charges were computed on the worth of the fresh and spent fuel respectively, assuming pre-irradiation and post-exposure holdup times of 150 days each.

Burnup. Unit feed costs as a function of enrichment were based on the current AEC cost schedule. Credit for the reprocessed uranium similarly was based on the enrichment with no penalty assessed for the presence of the  $^{236}\text{U}$  isotope. Fissile plutonium was assumed to sell at \$10/g.

Fabrication Unit Costs. Rough estimates of fabrication unit costs, based on extrapolations from previous HTGR cost data generated for the advanced converter study, were supplied by A. L. Lotts and T. N. Washburn.<sup>11</sup> In these estimates an amortization rate of 22% was assumed for fabrication-plant capital investment. The 13.0-in. lattice was examined, first assuming a small-fuel-hole cluster and then a large-fuel-hole cluster. The uncoated  $\text{UO}_2$  was assumed to be present in pelletized form. Unit costs were estimated for three values of throughputs: 170, 400, and 1100 MT/yr. The results are plotted in Fig. 2.

The large increase in the small-fuel-hole unit costs over those of the large-fuel-hole unit costs is attributable to two causes. The first is simply the much smaller amount of  $\text{UO}_2$  per unit length of fuel element.\* The second is the result of choosing pellets as the fuel form. A greater number of pellets per unit length of fuel element are required in the small fuel holes because the height-to-diameter ratio of a pellet is optimally held at one.

A change in cell dimensions for a given fuel-hole size would also affect the hardware unit costs inasmuch as more graphite would have to be

---

\*"Fuel element" should be understood as the whole cell.

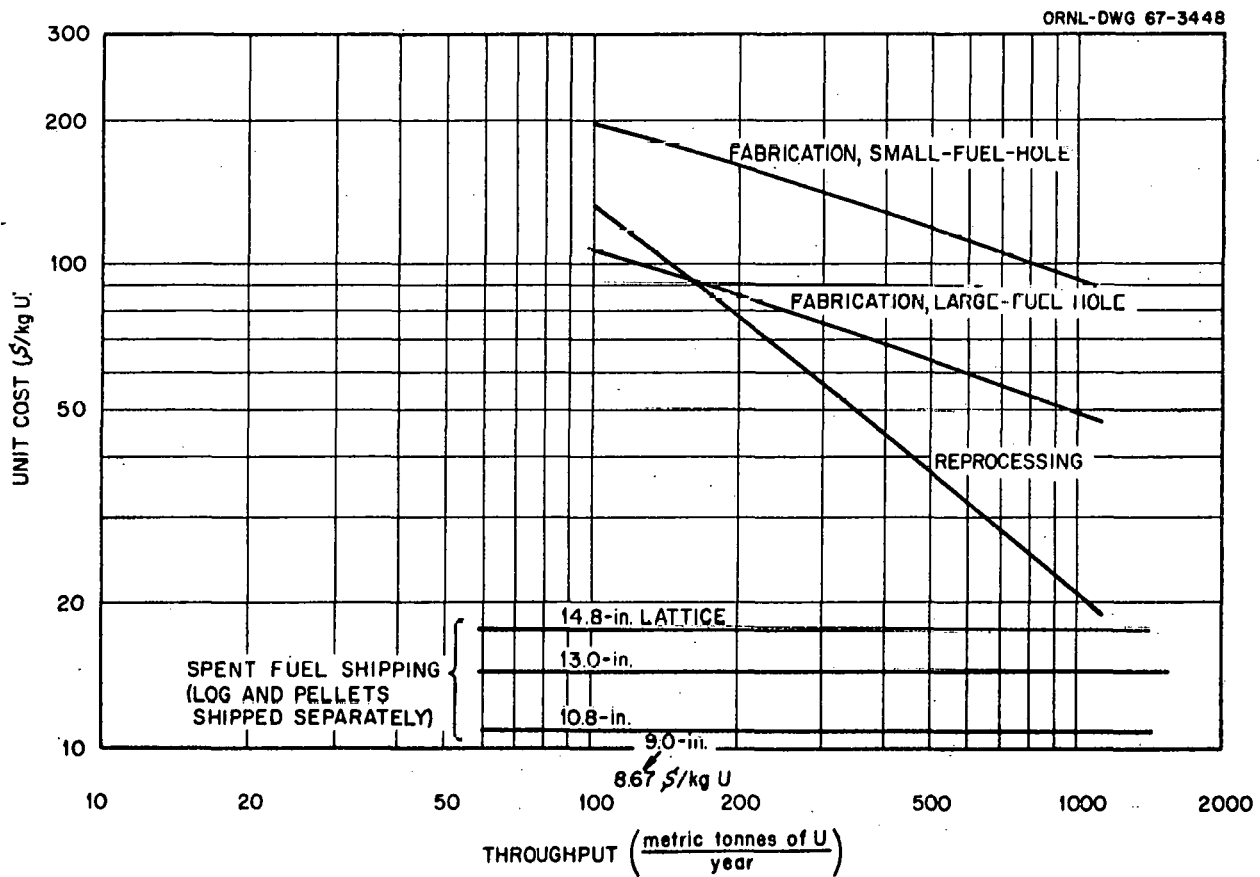


Fig. 2. Fabrication, Reprocessing and Shipping Unit Costs for Graphite Log Containing Uncoated  $\text{UO}_2$  Pellets.

purchased per kg of uranium. However, this effect is less important since the material cost of the bulk graphite is small relative to the total hardware cost of the finished product. No adjustment of fabrication unit costs for different size lattices has been applied.

Shipping Unit Costs. R. Salmon calculated the unit shipping costs for spent fuel.<sup>12</sup> In the most economical procedure, the pellets are removed and shipped separately from the log. Further cost reductions may be gained by cutting the log into parts.

The calculations were carried out for the 13-in. cell. Costs associated with the shipment of the graphite were extrapolated to other size cells by scaling the 13-in. value by the square of the ratio of lattice pitches (i.e.,  $[9/13]^2$ ,  $[10.8/13]^2$ , etc.). The unit costs associated with the shipment of spent  $UO_2$  were constant for all lattices. Added costs for canning the  $UO_2$  and the graphite for separate shipment were estimated at \$1/kg U each. The unit costs for spent fuel shipment are plotted in Fig. 2. Fresh-fuel shipping charges were estimated at \$2/kg U for the small-fuel-hole lattices and \$1/kg U for the large-fuel-hole lattices.

Reprocessing Unit Costs. Estimates of reprocessing costs were supplied by J. T. Roberts.<sup>13</sup> In accordance with the most economical shipping procedures, the  $UO_2$  pellets and graphite log are assumed to arrive separately at the reprocessing plant, whereupon the log is disposed of by dissolution in nitric acid. A single-purpose processing-plant industry and an amortization rate of 22% were also assumed.

Unit costs were computed for three cases, corresponding to throughputs of 170, 400, and 1100 MT of fuel per year. The results are plotted in Fig. 2.

Storage Unit Costs. In the event that no economic advantage accrues from reprocessing of fuel, the fuel is shipped elsewhere and stored. A storage charge of \$2.50/kg U was assessed therefore in "throwaway cycle" calculations. The same shipping charges as those used for reprocessed fuel were assumed.

Interest on Working Capital. Interest charges on the working capital required for fabrication, shipping, and reprocessing were computed using

the present-worth method. Quarterly payments and collection of revenue were assumed to occur together. The time period for retirement of the fabrication debt was taken as 60 days plus the fuel residence time. The time period for accumulation of interest on the shipping and reprocessing debts was taken as the fuel residence time plus 120 days.

### 3. Results

Conversion Ratios and Burnup. Tabulations of conversion ratios and burnups for the different lattices are given in Part 1 of Appendix C. Graphical representations of various relations among the independent variables, enrichment and lattice pitch, and the dependent variables,  $k_{\text{eff}}$ , burnup, and conversion ratio, are presented in Figs. 3, 4, and 5.

In Fig. 3 burnup is plotted as a function of lattice pitch with enrichment as a parameter. The small-fuel-hole burnup curves are observed to pass through mild maximums at lattice pitches in the vicinity of 11.5 to 12 in. The curves are quite flat; only the 9-in. lattices of those investigated yielded appreciably smaller burnups than the maximum values. Compared to the small-fuel-hole reactors the large-fuel-hole reactors at the same enrichment and lattice pitch generally show slightly higher burnups (an exception is the 5%-enriched, 13-in.-pitch case).

In Fig. 4 the conversion ratios are displayed functionally in the same manner as burnup. Conversion ratios varied between 0.43 and 0.70 for the small-fuel-hole clusters, and between 0.54 and 0.72 for the large-fuel-hole clusters. The usual trends are observed: conversion ratio decreasing with increasing enrichment for a given lattice pitch and decreasing with increasing lattice pitch for a given enrichment.\*

In Fig. 5 curves of constant initial  $k_{\text{eff}}$ , burnup, and conversion ratio for the small-fuel-hole reactors are plotted in the two-dimensional space of lattice-pitch and enrichment. The curves of conversion ratios 0.60 and 0.65 may not be extrapolated into regions much beyond lattice pitches of 14 and 12 in., respectively, because of criticality limitations.

---

\* Conversion ratio is defined here as the ratio of captures in the fertile nuclides to the absorptions in the fissile nuclides based on the steady-state concentrations of the nuclides.

ORNL-DWG 67-3449

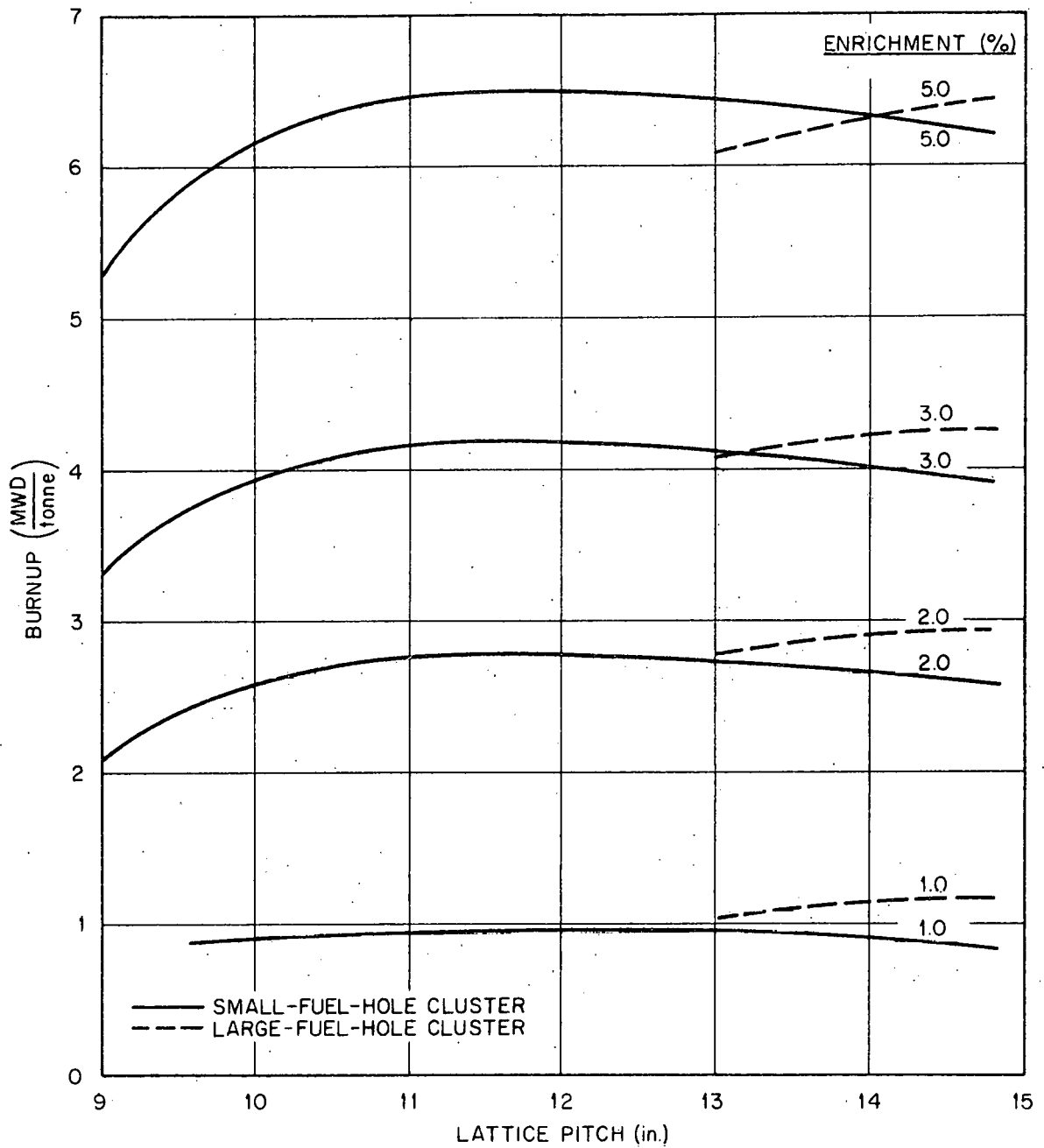


Fig. 3. Burnup Versus Lattice Pitch and Enrichment.

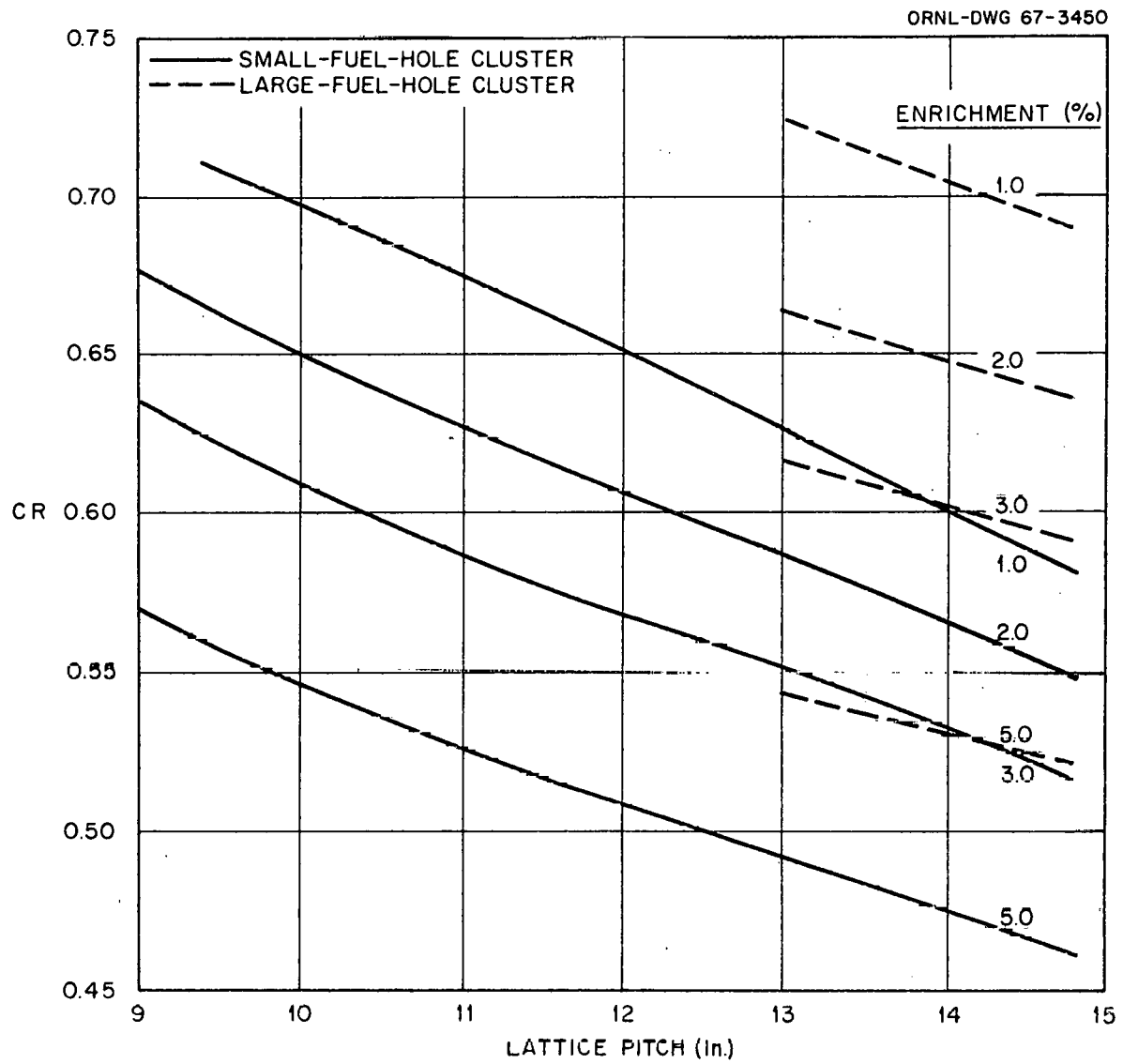


Fig. 4. Conversion Ratio Versus Lattice Pitch and Enrichment.

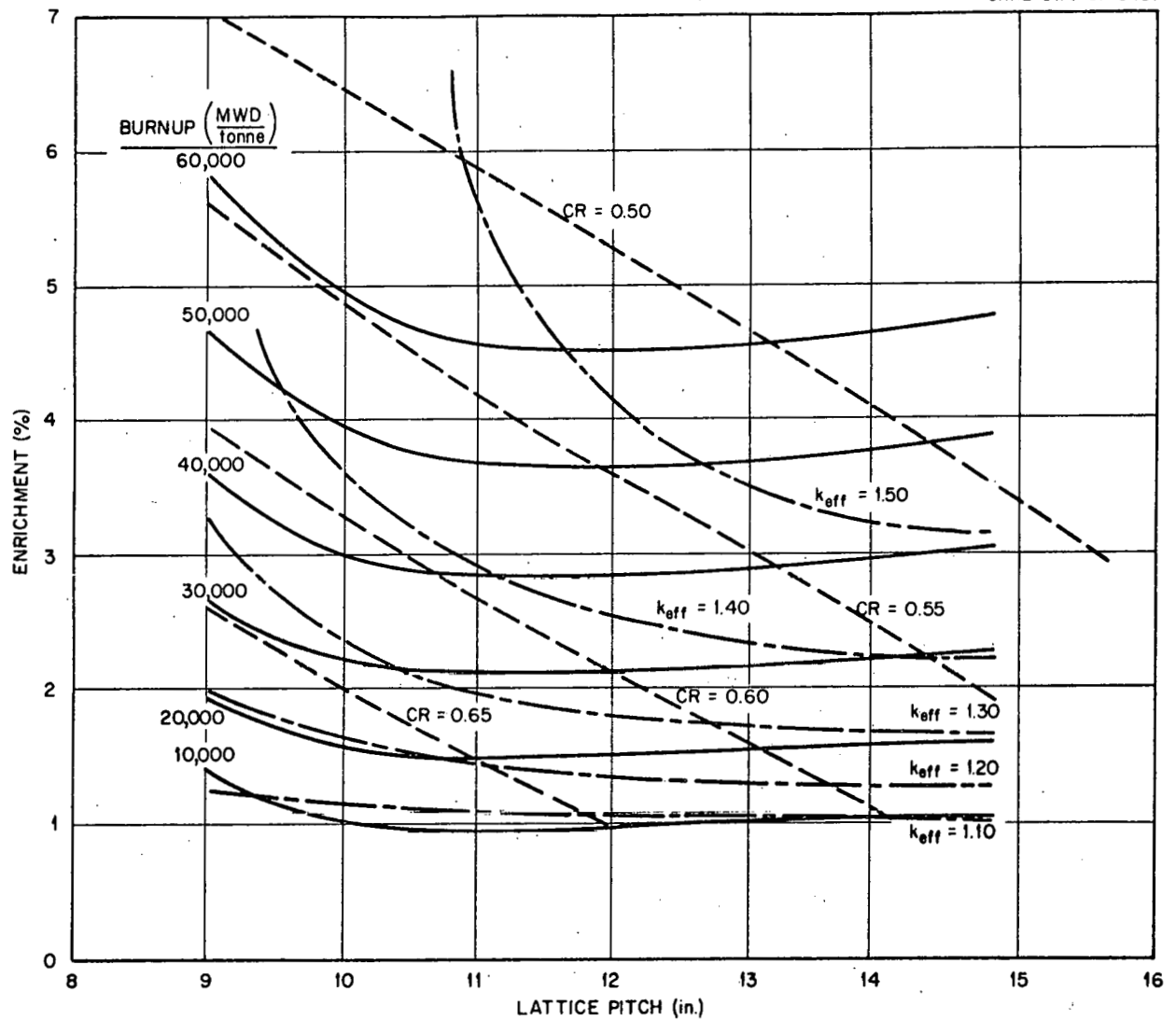


Fig. 5. Curves of Constant Initial  $k_{eff}$ , Conversion Ratio, and Burnup in Lattice Pitch Enrichment Space.

Fuel-Cycle Costs. Total fuel-cycle costs for each reactor are presented in Table 6. Both spent-fuel reprocessing and "throwaway" costs are exhibited and it is apparent that little difference exists between them. The study shows that it is somewhat more economically advantageous to reprocess and sell the plutonium and remaining  $^{235}\text{U}$  for credit in the large-fuel-hole cases. This is also true for all 2, 3, and 5% enrichment cases of the small-fuel-hole lattices, with the exception of the 9-in. lattice. It is slightly more advantageous to "throwaway" (i.e., store) in the 9-in. lattice cases and in the 1%-enriched cases of the other small-fuel-hole lattices.

A breakdown of the component costs are tabulated in Part 2 of Appendix C. In addition, the specific power (thermal kilowatts per gram of equilibrium fissile material) and the throughputs (metric tons of U per year) are given. In computing the "throwaway" total costs, the reprocessing and credit (a negative number) charges are omitted and the storage charge is added.

The subsequent discussion of Figs. 6, 7, and 8 will be restricted to the reprocessed-fuel cases in order to compare the economic effects of enrichment, lattice-pitch, and fuel-hole variation on the same basis. Moreover, the minimum total cost of the study, as well as costs closest to the minimum, are those of reprocessed fuel.

In Fig. 6 the total fuel-cycle cost and the component costs for the small-fuel-hole, 13-in. lattice, are plotted against enrichment. In Fig. 7 similar curves are drawn for the large-fuel-hole, 13-in. lattice. Hence, a comparison of the two figures shows the considerable effect of fuel-hole size on both the magnitude and enrichment-dependence of fuel-cycle cost. (In both figures total fuel-cycle costs for the remaining lattices are added as dashed-line curves for the sake of comparison.)

The nearly factor-of-two higher, unit fabrication costs of the small-fuel lattices are sufficient to increase the total costs above those of the large-fuel-hole lattices in the 1 to 2% enrichment range. This, of course, is the range where fabrication costs are at their highest because of the large throughputs. At enrichments higher than 2%, the large core-inventory charges of the large-fuel-hole lattices, in combination with

Table 6. Total Fuel-Cycle Costs [mills/kwhr(e)]

Lattice Pitch (in.)	Enrichment (%)							
	1		2		3		5	
	$C_T^a$	$C_{Th}^b$	$C_T$	$C_{Th}$	$C_T$	$C_{Th}$	$C_T$	$C_{Th}$
9.0 (S)			1.545	1.682	1.545	1.652	1.760	1.879
10.8 (S)	1.783	1.864	1.348	1.323	1.359	1.330	1.497	1.474
13.0 (S)	1.811	1.829	1.371	1.324	1.365	1.314	1.440	1.398
14.8 (S)	2.033	2.062	1.451	1.393	1.408	1.349	1.477	1.428
13.0 (L)	1.292	1.406	1.226	1.259	1.409	1.440	1.840	1.886
14.8 (L)	1.225	1.265	1.160	1.163	1.296	1.301	1.615	1.631

<sup>a</sup>Fuel reprocessed and sold for credit.

<sup>b</sup>Fuel not reprocessed but stored.

ORNL-DWG 67-3452

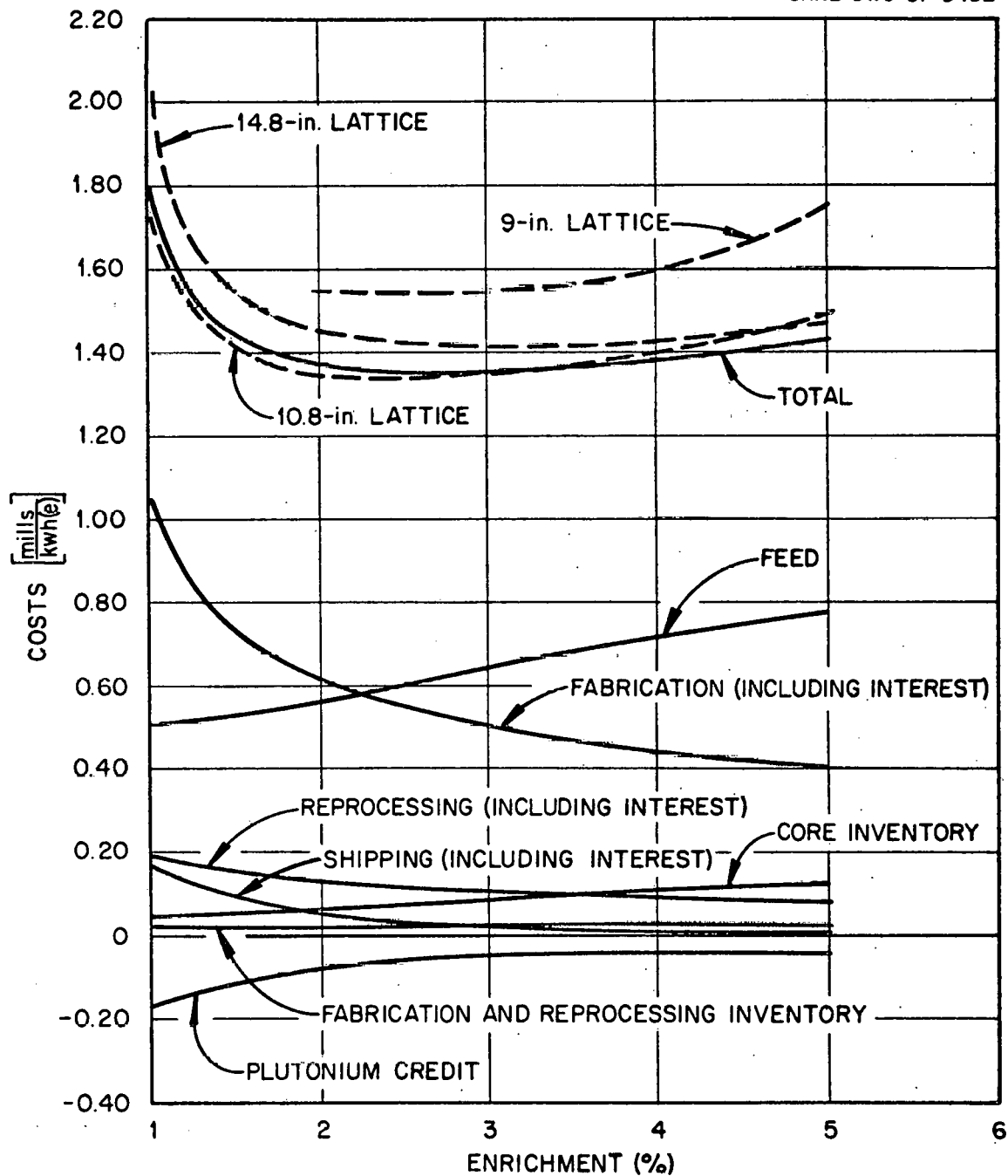


Fig. 6. Component Fuel-Cycle Costs Versus Enrichment (Small-Fuel-Hole, 13-in. Lattice).

ORNL-DWG 67-3453

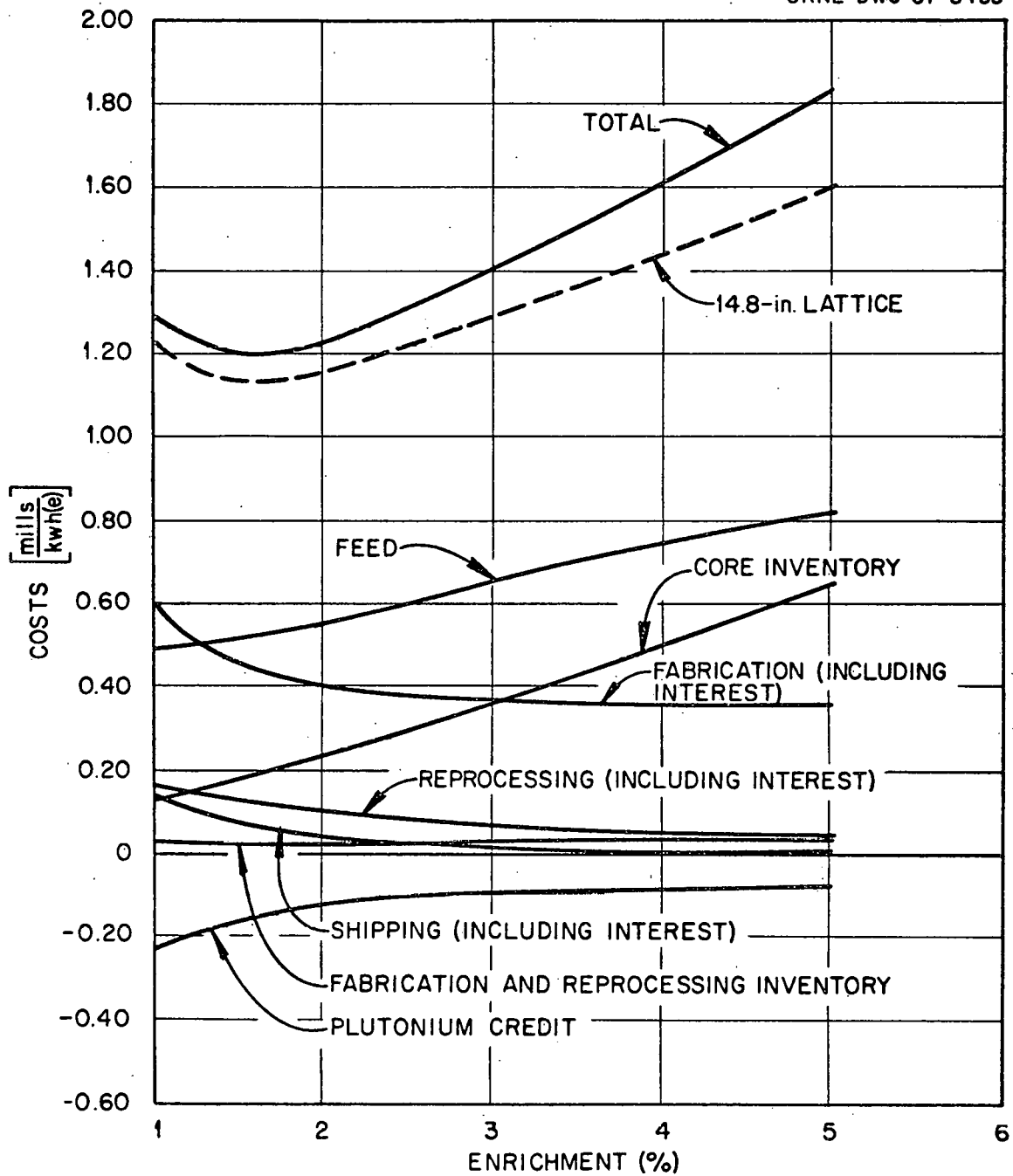


Fig. 7. Component Fuel-Cycle Costs Versus Enrichment (Large-Fuel-Hole, 13-in. Lattice).

ORNL-DWG 67-3454

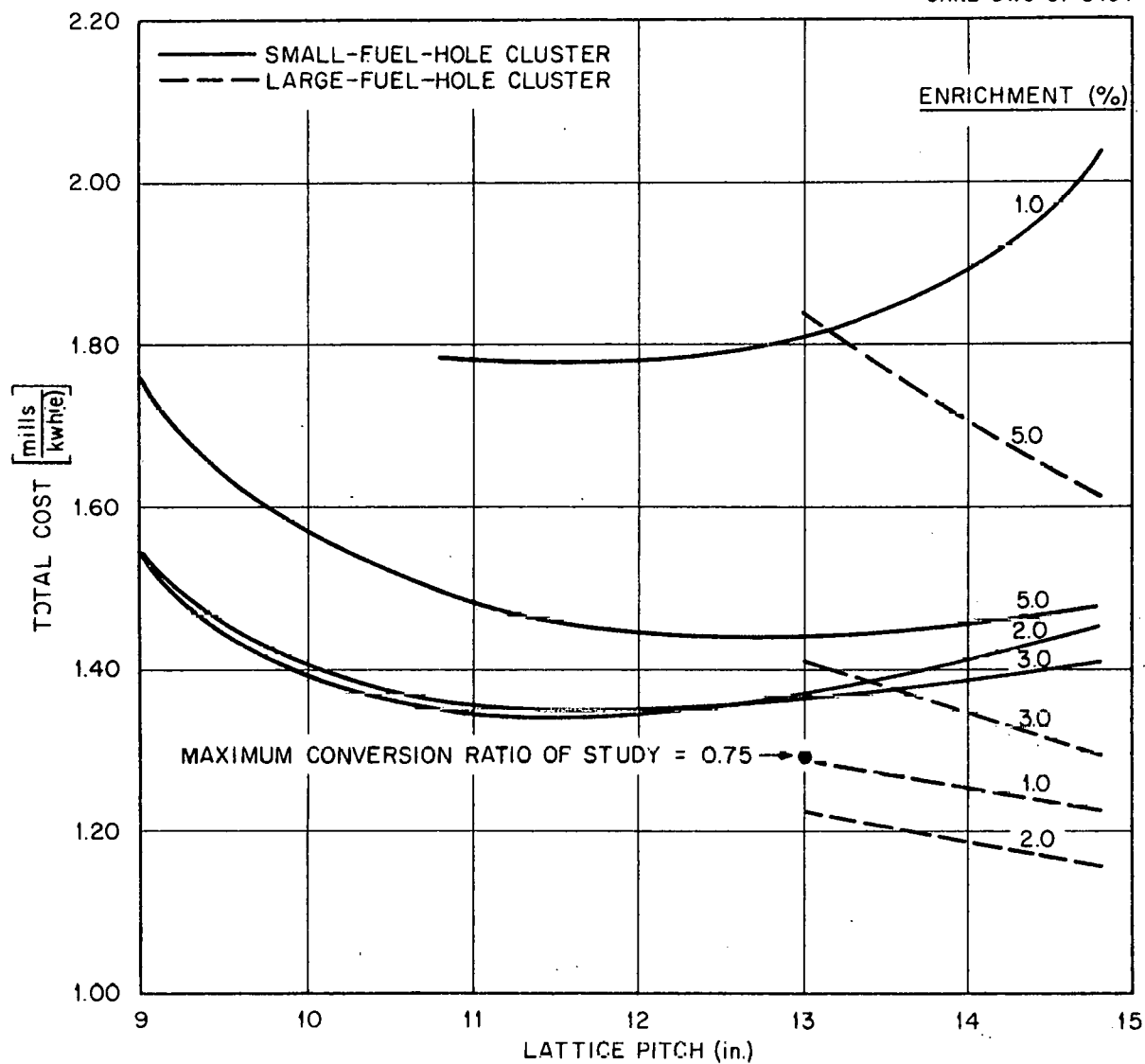


Fig. 8. Total Fuel-Cycle Costs Versus Lattice Pitch and Enrichment.

little further reduction in fabrication cost, drives the total costs of these lattices well beyond those of the small-fuel-hole lattices.

Although only the component costs of the 13-in. lattices are compared, the comparison is similar for the other lattices. The study shows that the cost-minimizing enrichment moves to lower values when the fuel-hole size is increased. In the small-fuel-hole lattices the minimizing enrichment generally lies between 2.5 and 3.0%, whereas in the large-fuel-hole lattices it lies between 1.5 and 2.0%.

In Fig. 8 the total fuel-cycle costs for all lattices investigated are plotted as a function of lattice pitch, with enrichment as a parameter. Of the points actually calculated the large-fuel-hole lattice of 2% enrichment and 14.8-in. pitch provides the lowest total cost: 1.160 mills/kwhr(e). Its conversion ratio is 0.637. However, another interesting case, which is only slightly higher in cost, is the large-fuel-hole lattice of 1% enrichment and 13-in. pitch. Here the maximum conversion ratio of the study, 0.724, obtains with an associated cost of 1.292 mills/kwhr(e).

Of the small-fuel-hole lattices actually calculated a minimum (throwaway) cost of 1.319 mills/kwhr(e) is reached at 3% enrichment and 13.0-in. pitch. The associated conversion ratio is 0.551. The cost minimizing lattice pitches for all small-fuel-hole curves of constant enrichment correspond fairly closely with the burnup maximizing lattice pitches (Fig. 3).

#### IV. CONCLUSIONS

An analysis of fuel-cycle costs associated with a limited number of combinations of lattice pitch, enrichment and fuel-hole size has been carried out for a heterogeneous, unclad,  $\text{UO}_2$ -graphite reactor. A lowest value of 1.16 mills/kwhr(e) was found for the case whose characteristics are summarized in Table 7.

Unit fabrication costs, decreasing by nearly a factor of two when large-fuel holes are substituted for small-fuel holes, played the primary role in determining a large-fuel-hole reactor as the minimum-cost case.

Table 7. Summary of Characteristics of Lowest Cost Lattice of this Study

---

Fuel	UO <sub>2</sub>
Initial enrichment, %	2.0
Lattice pitch, in.	14.8
Diameter of fuel hole, in.	0.576
Initial carbon-to- <sup>235</sup> U atom ratio	6257
Equilibrium carbon-to-fissile atom ratio	13,451
Power density, w/cm <sup>3</sup> cell	1.98
Initial specific power, w/g total U	8.28
Equilibrium, fissile specific power, w/g fissile	897.0
Equilibrium conversion ratio	0.637
Burnup	
Cycle time, full-power days	3554
Fissions per initial fissile atom	1.556
Mwd/MT	29,410
Fabrication plant throughput, MT U/year	373.2
Unit cost fabrication, \$/kg U	69.8
Unit cost reprocessing, \$/kg U	47.5
Unit cost shipping, \$/kg U	18.8
Fuel-cycle costs, mills/kwhr(e)	
Fabrication (including interest)	0.397
Processing (including interest)	0.095
Shipping (including interest)	0.041
Uranium feed	0.521
Core inventory	0.171
Fabrication and reprocessing inventory	0.024
Plutonium credit	(0.089)
Total	1.160

---

It should be recognized that the estimates of unit fabrication costs are of an extrapolated and approximate nature and apply to a fuel element which is the lattice cell itself. The difficult question of whether the graphite must necessarily be replaced every fuel cycle, and if not, what cost reductions would be gained, was not taken up here. But the answer would certainly bear on the minimum fuel-cycle cost of this type of reactor.

The influence of unit-fabrication-cost assumptions on the optimum lattice characteristics and minimum cost is further illustrated by comparison with a previous paper.<sup>9</sup> There, based on the same conceptual lattices and physics of this study, and the physics of a gas-cooled, semi-homogeneous, UC-graphite reactor utilizing more highly enriched uranium, it was shown that the minimum (equilibrium) fuel-cycle costs for both reactor types were obtained for throwaway cycles and were approximately the same: 0.92-0.94 mills/kwhr(e). The unit fabrication cost vs throughput curve (Fig. 5, Ref. 9) was assumed to be the same for the semi-homogeneous model and for both large and small-fuel-hole lattices of the heterogeneous type. The optimum heterogeneous lattice using these unit costs was found to be the small-fuel-hole lattice of 13.0-in. pitch and 2% enrichment in contrast to the result of this study. The characteristics and fuel-cycle costs for the minimum cost, semi-homogeneous and heterogeneous cases of Ref. 9 are repeated here in Table 8.

#### ACKNOWLEDGMENTS

I would like to thank R. S. Carlsmith and W. E. Thomas for their advice and help in orienting me in the field of reactor economics analysis.

Table 8. Summary of Characteristics of Ref. 9, Minimum Cost, Semi-Homogeneous and Heterogeneous HTGR's; for Low-Enriched Uranium Fuel Using Semi-Homogeneous Fabrication Unit Costs<sup>a</sup>

	Semi-Homogeneous <sup>b</sup>	Heterogeneous
Fuel	UC	UO <sub>2</sub>
Initial enrichment, %	8.09	2.0
Lattice pitch, in.	N.A.	13.0
Diameter of fuel hole, in.	N.A.	0.375
Initial carbon-to- <sup>235</sup> U atom ratio	10,000	11,254
Equilibrium carbon-to-fissile atom ratio	24,013	25,458
Power density, w/cm <sup>3</sup>	5.0	2.58
Equilibrium fissile specific power, w/g fissile	6060	2230
Equilibrium conversion ratio	0.60	0.59
Burnup		
Cycle time, full-power days	573	1400
Fission per initial fissile atom	1.52	1.44
Mwd/MT	116,350	27,300
Fabrication plant throughput, MT/year	94.3	403.0
Unit cost fabrication, \$/kg U <sup>c</sup>	86.00	58.50
Unit cost reprocessing, \$/kg U <sup>c</sup>	190.00	53.00
Fuel-cycle cost, mills/kwhr(e)		
Fabrication (including interest)	0.085	0.270
Uranium feed	0.753	0.561
Shipping plus storage	0.006	0.022
Core inventory	0.048	0.066
Fabrication inventory	0.031	0.023
Total	0.923	0.942

<sup>a</sup>No recycle, no reprocessing.

<sup>b</sup>Based on reoptimized fuel compositions for spent fuel discard. Numbers here consequently differ at times from numbers in Tables 2 and 3 of Ref. 9.

<sup>c</sup>Based on curves of Fig. 5 of Ref. 9. It is interesting to note that the fabrication unit cost for the heterogeneous case in this table would be much higher if the value in Fig. 2 of this study were used: 129 \$/kg U. (Reprocessing unit cost would be 45 \$/kg U.)

## REFERENCES

1. R. S. Carlsmith and W. E. Thomas, LTM: An IBM 7090 Multigroup Burnup Code for Equilibrium Reactor Fuel Cycles, unpublished computer code.
2. G. D. Joanou and J. S. Dudek, GAM-1: A Consistent  $P_1$  Multigroup Code for the Calculation of Fast Neutron Spectra and Multigroup Constants, USAEC Report GA-1850, General Atomic, June 28, 1961.
3. G. D. Joanou and J. S. Dudek, GAM-2: A  $B_3$  Code for the Calculation of Fast-Neutron Spectra and Associated Multigroup Constants, USAEC Report GA-4265, General Atomic, September 16, 1963.
4. H. Honeck, THERMOS: A Thermalization Transport Theory Code for Reactor Lattice Calculations, USAEC Report BNL-5826, Brookhaven National Laboratory, September 1961.
5. E. Hellstrand, Measurements of the Effective Resonance Integral in Uranium Metal and Oxide in Different Geometries, J. Appl. Phys., 28(13): 1493 (December 1957).
6. A. Sauer, Approximate Escape Probabilities, Nucl. Sci. Eng., 16(3): 329 (July 1963).
7. Reactor Physics Constants, 2nd ed., USAEC Report ANL-5800, Argonne National Laboratory, July 1963.
8. M. W. Rosenthal et al., A Comparative Evaluation of Advanced Converters, USAEC Report ORNL-3686, Oak Ridge National Laboratory, January 1965.
9. R. S. Carlsmith, C. M. Podeweltz, and W. E. Thomas, Fuel-Cycle Cost Comparison for High-Temperature Gas-Cooled Reactor Fuels, paper presented at the Symposium on Fuel Cycles of High-Temperature Gas-Cooled Reactors, Brussels, June 1965; also issued as ORNL-TM-1112.
10. G. Samuels and M. E. Lackey, Oak Ridge National Laboratory, unpublished calculations.
11. A. L. Lotts and T. N. Washburn, Oak Ridge National Laboratory, personal communication to C. M. Podeweltz, Oak Ridge National Laboratory.
12. R. Salmon, Oak Ridge National Laboratory, personal communication to C. M. Podeweltz, Oak Ridge National Laboratory.
13. J. T. Roberts, Oak Ridge National Laboratory, personal communication to C. M. Podeweltz, Oak Ridge National Laboratory.

14. Doppler Coefficient for  $^{238}\text{U}$ , Power Reactor Technology, 2(2): 14 (March 1959).
15. Reactor Physics Constants, 2nd ed., USAEC Report ANL-5800, Table 4.24, p. 279, Argonne National Laboratory, July 1963.
16. J. Chernick and Russel Vernon, Some Refinements in the Calculations of Resonance Integrals, Nucl. Sci. Eng., 4(5): 649 (1958).
17. W. Rothenstein, Collision Probabilities and Resonance Integrals for Lattices, USAEC Report BNL-563 (T-151), Brookhaven National Laboratory, June 1959.
18. L. W. Nordheim, The Theory of Resonance Absorption, Symposium Appl. Math.; Vol. XI, p. 58 (1961).
19. B. Pershagen, G. Andersson, and I. Carlvik, Calculation of Lattice Parameters for Uranium Rod Clusters in Heavy Water and Correlation with Experiments, Proceedings of the Second United Nations International Conference on the Peaceful Uses of Atomic Energy, P/151, Vol. 12, p. 341 (1958).
20. K. M. Case, F. de Hoffman, and G. Placzek, Introduction to the Theory of Neutron Diffusion, Vol. I, Government Printing Office, Washington, D. C., 1953.

## APPENDIX A

## DETERMINATION OF THE DANCOFF FACTOR

1. Application of Experimental Data

In Ref. 5 Hellstrand presents two empirical fits to the effective resonance integral of  $^{238}\text{U}$  in  $\text{UO}_2$  rods, one a linear function of the effective surface-to-mass ratio of the oxide, the other varying as the square root of the ratio. The former has been used in this study, i.e.,\*

$$\text{RI} = 11.6 + 22.8 \left( \frac{S_{\text{eff}}}{M} \right)_{\text{UO}_2} \quad (0.2 \leq \frac{S_{\text{eff}}}{M} \leq 0.7) . \quad (\text{A.1})$$

In the case of cluster geometry the whole cluster is treated as a rod which has a mass equal to the sum of the individual fuel masses. The effective surface area, as defined by Hellstrand, is taken to be the rubber band area (i.e., the area defined by a rubber band stretched around the cluster), augmented by an internal surface area contribution which depends on the geometry and the internal moderator of the cluster. The augmentation is negligible if there is no internal moderator. In this study, due to the presence of graphite, the internal surface area contribution amounted to roughly 7% of  $S_{\text{eff}}$  for the small-fuel-hole cluster and 13% of  $S_{\text{eff}}$  for the large-fuel-hole cluster.

Equation (A.1) holds for room temperature conditions. The temperature dependence given on page 14 of Ref. 14 was applied to estimate resonance integrals at  $727^\circ\text{C}$  ( $1000^\circ\text{K}$ ). For  $T$  in  $^\circ\text{C}$  Hellstrand's formula becomes

$$\begin{aligned} \text{RI}(T) = & 11.6[1.0 + 10^{-5}(T - 20)] \\ & + 22.8[1.0 + 3.1 \times 10^{-4}(T - 20)] \left( \frac{S_{\text{eff}}}{M} \right)_{\text{UO}_2} . \quad (\text{A.2}) \end{aligned}$$

---

\*The linear fit has been used in the large-fuel-hole cluster even though the  $S_{\text{eff}}/M$  ratio is 0.15. This was done to maintain consistency in the physics comparison of large- and small-fuel-hole clusters. The study originally was projected only for the small-fuel-hole lattices which had an  $S_{\text{eff}}/M$  ratio of 0.33.

The value obtained for RI is then used in the following standard formula to compute the resonance-escape probability for  $^{238}\text{U}$  in  $\text{UO}_2$ ,

$$p = \exp - \left[ \frac{(RI) N_{28}}{N_c (\xi \sigma_s)_c + N_o (\xi \sigma_s)_o + N_{28} (\xi \sigma_s)_{28}} \right], \quad (\text{A.3})$$

where  $N_{28}$ ,  $N_c$ , and  $N_o$  are the homogenized cell atomic densities for  $^{238}\text{U}$ , carbon, and oxygen; and  $(\xi \sigma_s)_{28}$ ,  $(\xi \sigma_s)_c$ , and  $(\xi \sigma_s)_o$  are their respective slowing-down powers.

By using these last two formulas, one obtains an effective resonance integral for  $^{238}\text{U}$  at  $1000^\circ\text{K}$  exclusive of the  $1/v$  portion, and exclusive of all neutron absorption above  $\sim 100$  kev. Table 1, on page 6, summarizes the results obtained from calculations of resonance integrals and resonance-escape probabilities using Eqs. (A.2) and (A.3). The calculations were done for the 9-in. lattice in the small-fuel-hole case, and the 13-in. lattice in the large-fuel-hole case. These were the lattices for which the purely theoretical calculations of resonance-escape probabilities were made.

## 2. Theoretical Calculations

Both the GAM-1 (Ref. 2) and GAM-2 (Ref. 3) codes contain auxiliary computer routines which solve the resonance absorption problem for those nuclides specified as "resonance absorbers," and prepare appropriately weighted microscopic absorption cross sections for a given energy grid. In the present study the resonance treatments of  $^{235}\text{U}$ ,  $^{240}\text{Pu}$ , and  $^{242}\text{Pu}$  were assigned to the GAM-1 code, while the more crucial matter of  $^{238}\text{U}$  resonance absorption was handled by the GAM-2 code. All group-averaged cross sections for the rest of the nuclides, as well as the scattering cross sections for  $^{238}\text{U}$ , were calculated by the GAM-1 code. GAM-2 supplied only the fission and absorption cross sections of  $^{238}\text{U}$ .

The investigation into the best way of estimating the Dancoff factor — "best" being taken in the sense described on page 5 — was carried out utilizing the GAM-2 code exclusively.  $^{238}\text{U}$  dioxide was specified as the fuel, graphite as the moderator, and the small-fuel-hole

cluster geometry was assumed. Three different methods of calculating the Dancoff factor (C) were tried.\*

In the first, the rational approximation,  $C (= C_R)$  was computed for an infinite array from the expression:

$$C_R = \frac{1}{1 + \Sigma_m \bar{\ell}_m}, \quad (\text{A.4})$$

where  $\Sigma_m$  is the effective, macroscopic total cross section averaged over the resonance range for the moderator within the cluster. (In this study the pure graphite cross section,  $\sim 0.39 \text{ cm}^{-1}$ , was weighted by the ratio of graphite volume within the cluster to graphite plus coolant volume within the cluster.)  $\bar{\ell}_m$  is the mean chord length of the cluster moderator and was taken to be

$$\bar{\ell}_m = 2R_0 \frac{V_1}{V_0},$$

where  $R_0$  is the radius of the fuel hole,  $V_0$  is the fuel volume in the cluster, and  $V_1$  is the non-fuel volume in the cluster.

In the second method, Sauer's approximation,<sup>6</sup>  $C (= C_S)$  was computed for an infinite array according to the formula:

$$C_S = \frac{\exp[-\tau \Sigma_m \bar{p}_m]}{1 + (1 - \tau) \Sigma_m \bar{\ell}_m}, \quad (\text{A.5})$$

where  $\tau$  is a geometric index, dependent upon the lattice arrangement. For the hexagonal lattice of this study,

$$\tau_{\text{hex}} = \frac{\left[ \sqrt{\pi/2} \sqrt{3} \sqrt{1 + V_1/V_0} - 1 \right]}{(V_1/V_0)} - 0.12.$$

---

\*Reference to Dancoff factor calculations in the following discussion implies only that the interaction between rods within a cluster is being considered.

In the last method recourse was had to the tables of the Dancoff-Ginsburg factor appearing on pages 283-91 in Ref. 7, where each entry gives the fractional reduction in flux upon the surface of a rod, of radius  $\rho$  cm, by an identical rod  $d$  cm away - the intervening moderator medium characterized by total cross section  $\Sigma_m$ . Factors for the nearest neighbor ( $d$  cm away) and the next-nearest neighbor ( $\sqrt{3} d$  cm away) were computed. Each of these factors was multiplied respectively by the number of neighbors of that type which the rod would see from its particular position in the cluster, the results added and further multiplied by the number of rods having identical positions. These last results were then added and the total divided by nineteen to give the average Dancoff factor for the cluster. Letting  $C_n$  denote the nearest-neighbor factor between two rods, and  $C_{nn}$  the next-nearest-neighbor factor, the average Dancoff factor by this method ( $\bar{C} = \bar{C}_D$ ) is written in brief as,

$$\bar{C}_D = \frac{84 C_n + 60 C_{nn}}{19} . \quad (A.6)$$

Factors computed from these three formulas and also a factor of zero were supplied to the GAM-2 code. The 9-in. lattice homogenized data were chosen for the test cases. From the resulting output of group-averaged cross sections, the  $^{235}\text{U}$  resonance-escape probability associated with each Dancoff factor was computed by multiplying together the individual escape probabilities for each group, from group three to group nine,\* i.e.,

$$p(C) = \prod_{i=3}^9 \left[ \frac{\Sigma_{os}^h(C)}{\Sigma_{rem}^h(C)} \right]_i , \quad (A.7)$$

where  $\Sigma_{os}^h$  is the homogeneous macroscopic outscattering cross section and  $\Sigma_{rem}^h$  is the homogeneous macroscopic removal cross section.

The resonance-escape probability associated with  $C = 0$ ,  $p_0$ , was combined with the resonance-escape probabilities associated with  $C_R$  and

---

\*Group three begins at 183 kev and group nine ends at 5.04 ev.

$C_S$ ,  $p_R$  and  $p_S$  respectively, in the following manner in order to produce finite cluster-averaged probabilities for these two approximations:

$$\bar{p}_{R \text{ or } S} = \frac{14p_{R \text{ or } S} + 5p_o}{19} \quad . \quad (A.8)$$

The cluster-averaged Dancoff factors via the rational or Sauer approximations,  $\bar{C}_R$  and  $\bar{C}_S$ , were then obtained by interpolation from a plot of resonance-escape probability vs Dancoff factor based on the GAM-2 results..

It is observed (Table 2) that the use of the rational approximation to the Dancoff factor results in an overestimate of the resonance-escape probability, if the Hellstrand value is accepted as the best estimate. This is consistent with previous findings<sup>16,17,18</sup> that the escape probability from a medium — in this case the cluster moderator — is underestimated and transmission probability overestimated by the rational approximation; hence the shadowing effect is overestimated. Last of all it is observed that the use of the Dancoff-Ginsburg tables of Ref. 16 provides a Dancoff factor in good agreement with the Hellstrand inferred value.

## APPENDIX B

## HETEROGENEITY OF THE FAST EFFECT

If intra-cluster moderation is small, the cluster may be homogenized and viewed as a single fuel rod. The fast effect is then calculated using a fuel collision probability based on the total macroscopic cross section of this composite rod. If intra-cluster moderation is not small, this procedure may still be used and the result further multiplied by the ratio of  $\epsilon$  for a single isolated pin to  $\epsilon$  for a homogenized unit cell associated with the pin, as suggested by Carlvik and Pershagen.<sup>19</sup> Alternatively, if intra-cluster moderation is appreciable the fast effect may be calculated using parameters which pertain to the individual fuel pin. In either case the magnitude of the pin-pin or cluster-cluster interaction effect may be measured by a fast-group Dancoff factor.

The development whose results are discussed here was generalized to permit pin-pin type calculations as well as cluster-cluster calculations, although in the latter case the intra-cluster moderator would be homogenized with fuel and cladding and all three would be considered as fuel in the heterogeneous calculations.

We assume there are available suitable energy-averaged cross sections for a one-fast-group model (as e.g., from the GAM codes). If moderator absorption and leakage effects are neglected the fast fission factors for the heterogeneous cell and its homogenized equivalent cell may be written as follows:

$$\epsilon_{\text{het}} = \frac{\alpha \Sigma_{\text{T}}^{\text{f}} - P_{\text{c}}^{\text{f}} (\Sigma_{\text{es}}^{\text{f}} + \chi \Sigma_{\text{a}}^{\text{f}}) + \beta}{\alpha \Sigma_{\text{T}}^{\text{f}} - P_{\text{c}}^{\text{f}} (\Sigma_{\text{es}}^{\text{f}} + \chi \nu \Sigma_{\text{f}}^{\text{f}})}, \quad (\text{B.1})$$

$$\epsilon_{\text{hom}} = \frac{(\Sigma_{\text{T}}^{\text{f}} - \Sigma_{\text{es}}^{\text{f}} - \chi \Sigma_{\text{a}}^{\text{f}}) V^{\text{f}} + \Sigma_{\text{os}}^{\text{im}} V^{\text{im}} + \Sigma_{\text{os}}^{\text{em}} V^{\text{em}} + \Sigma_{\text{os}}^{\text{l}} V^{\text{l}}}{(\Sigma_{\text{T}}^{\text{f}} - \Sigma_{\text{es}}^{\text{f}} - \chi \nu \Sigma_{\text{f}}^{\text{f}}) V^{\text{f}} + \Sigma_{\text{os}}^{\text{im}} V^{\text{im}} + \Sigma_{\text{os}}^{\text{em}} V^{\text{em}} + \Sigma_{\text{os}}^{\text{l}} V^{\text{l}}}. \quad (\text{B.2})$$

The superscripts "f", "im", "em", and "l" denote "fuel", "intra-cluster moderator", "extra-cluster moderator", and "cladding" respectively.

The subscripts "es", "os", "f", "a", and "T" on the macroscopic cross sections,  $\Sigma$ , denote "in-group transfer", "out-of-group transfer", "fission", "absorption", and "total" (i.e.,  $\Sigma_T^f = \Sigma_{es}^f + \Sigma_{os}^f + \Sigma_a^f$  and  $\Sigma_T^m = \Sigma_{es}^m + \Sigma_{os}^m$ ) reactions respectively.  $V$  denotes a volume fraction in the cell.  $\nu$  is the number of neutrons born per fast fission, and  $\chi$  is the fraction of these born into the fast group.

$P_c^f$  is the first-flight, Dancoff-corrected, fuel collision probability. To a good approximation  $P_c^f$  may be computed using Nordheim's formula<sup>18</sup>

$$1 - P_c^f = \frac{(1 - P_o^f)(1 - C)}{1 - C[1 - \Sigma_T^f \ell^f (1 - P_o^f)]}, \quad (B.3)$$

where

$P_o^f$  = the isolated-pin, first-flight collision probability tabulated in the tables of Case, de Hoffman and Placzek,<sup>20</sup>

$\ell^f$  = the mean chord length of the fuel pin,

$C$  = the fast-group Dancoff factor for fuel-to-fuel interaction.

In the case of pin-pin interaction where the pins are in clusters,  $C$  is a suitable average, calculated by an averaging procedure analogous to that described by Eq. (A.6) of Appendix A.

Both Eqs. (B.1) and (B.2) have been derived on the basis of defining  $\epsilon$  as the number of neutrons passing the fast-group's lower energy limit per neutron born from the non-fast fissions. The degradations from an infinite sequence of fast sub-cycle collisions are summed, weighted by  $\chi$ , and added to  $1 - \chi$  to obtain  $\epsilon$ .

In both derivations, an allowance is made for neutrons which suffer "in-group" scattering collisions in the moderator. Some of these therefore remain available to cause further fast fission in the fuel. In the heterogeneous case the quantities  $\alpha$  and  $\beta$  incorporate this allowance:

$$\alpha = 1 - (\Sigma_{es}^m / \Sigma_T^m) [P^m + (1 - P_c^f - P^m)(\chi \nu \Sigma_f^f + \Sigma_{es}^f) / \Sigma_T^f], \quad (B.4)$$

$$\beta = \chi (\Sigma_{es}^m / \Sigma_T^m) (1 - P_c^f - P^m) (\nu \Sigma_f^f - \Sigma_a^f). \quad (B.5)$$

When all moderator scattering is outscatter,  $\alpha = 1$ ,  $\beta = 0$ .  $\overline{\Sigma_{es}^m / \Sigma_T^m}$  is the average probability that a neutron stays within the fast group when it collides in a moderator material.  $P^m$  is the probability that a fast-group neutron present in the moderator will make its next collision in the moderator. Both are difficult to estimate when pin-pin interaction is being considered in cluster geometry and internal and external moderators are different materials. However in an array of clusters (when the "fuel rod" is a cluster-composite rod) or in an array of pins, with only void and one moderator filling the remaining volume,  $\Sigma_{es}^m / \Sigma_{es}^m$  becomes  $\Sigma_{es}^m / \Sigma_{es}^m$ ;  $P^m$  may be calculated from the reciprocity theorem:<sup>17</sup>

$$(1 - P_c^f) V^f \Sigma_T^f = (1 - P^m) V^m \Sigma_T^m. \quad (B.6)$$

Pin-pin interaction was calculated for the lattices of this study and the reciprocity theorem applied since internal and external moderators were identical. The utilization of GAM-1, fast-group, energy-averaged cross sections produced the results of Table 3.

In general, some corrective measure must be applied to homogeneous point calculations to insure that the proper fast effect is present. Since the usual multigroup, eigenvalue calculation does not concern itself with computing the fast effect per se but rather with the computation of  $k_{eff}$ , the implicit relation between the two, from the code's point of view, must be established.

We shall assume in order to isolate this relation that the homogeneous code, supplied with properly self-shielded resonance and thermal cross sections, computes the multiplication occurring below the fast group accurately. The code's  $k_{cutoff}$  value is obtained by summing the neutrons produced in each group which result from an initial total source of unity,

$$k_{eff}(\text{code}) = \sum_{i=1}^{i\text{-thermal}} (\nu \Sigma_f^{h,h})_i, \quad (B.7)$$

where the summation is over all energy groups  $i$ , and the superscript  $h$  denotes "homogeneous".

Let group 1 be the fast group, and rewrite the above expression in terms of productions in group 1 and productions in all other groups. We have assumed accurate multiplication by the code of those neutrons entering the groups below group 1. Therefore, this multiplication is designated as  $\eta pfP_\ell$ , where  $\eta$ ,  $p$ , and  $f$  are the familiar factors of the four-factor formula, and  $P_\ell$  is the non-leakage probability. The neutrons entering the groups below 1 are calculated by the code to be  $(\Sigma_{os}^h \phi^h)_1 + 1 - \chi_1$ , where  $\phi$  is the flux. The rewritten expression is thus

$$k_{\text{eff}}(\text{code}) = (\nu \Sigma_f^h)_1 + \eta pfP_\ell [(\Sigma_{os}^h \phi^h)_1 + 1 - \chi_1] . \quad (\text{B.8})$$

To ascertain the  $\epsilon$  implicit in  $k_{\text{eff}}(\text{code})$ , we define

$$k_{\text{eff}}(\text{code}) \equiv \epsilon(\text{code}) \eta pfP_\ell , \quad (\text{B.9})$$

then

$$\epsilon(\text{code}) = \frac{(\nu \Sigma_f^h)_1 \phi_1^h \epsilon(\text{code})}{k_{\text{eff}}(\text{code})} + (\Sigma_{os}^h \phi^h)_1 + 1 - \chi_1 . \quad (\text{B.10})$$

In a zero-dimensional code, whose source is normalized to one,

$$\phi_1^h = \frac{\chi_1}{(\Sigma_{os}^h)_1 + (\Sigma_a^h)_1} . \quad (\text{B.11})$$

Also

$$(\Sigma_{os}^h)_1 + (\Sigma_a^h)_1 = (\Sigma_T^h)_1 - (\Sigma_{es}^h)_1 .$$

Dropping the subscript "1", recognizing that all quantities except  $k_{\text{eff}}$  pertain to group 1, we find

$$\epsilon(\text{code}) = \frac{\Sigma_T^h - \Sigma_{es}^h - \chi \Sigma_a^h}{\Sigma_T^h - \Sigma_{es}^h - \frac{\chi \nu \Sigma_f^h}{k_{\text{eff}}(\text{code})}} . \quad (\text{B.12})$$

Since  $\Sigma^h = V_{\Sigma}^f \Sigma^f + V_{\Sigma}^{im} \Sigma^{im} + V_{\Sigma}^{em} \Sigma^{em} + V_{\Sigma}^l \Sigma^l$ ,

$$\epsilon(\text{code}) = \frac{\Sigma_T^f - \Sigma_{es}^f - \chi \Sigma_a^f + 1/V^f (V_{\Sigma_{os}}^{im} \Sigma^{im} + V_{\Sigma_{os}}^{em} \Sigma^{em} + V_{\Sigma_{os}}^l \Sigma^l)}{\Sigma_T^f - \Sigma_{es}^f - \frac{\chi \nu \Sigma_f^f}{k_{eff}(\text{code})} + 1/V^f (V_{\Sigma_{os}}^{im} \Sigma^{im} + V_{\Sigma_{os}}^{em} \Sigma^{em} + V_{\Sigma_{os}}^l \Sigma^l)} . \quad (\text{B.13})$$

$\epsilon(\text{code})$  is identical to the  $\epsilon_{hom}$  of Eq. (B.2) except for the  $k_{eff}(\text{code})$  appearing in the denominator. If  $k_{eff}(\text{code})$  is one or very close to one (as it is for the equilibrium condition) any alteration of constants which transforms  $\epsilon_{hom}$  into  $\epsilon_{het}$  will also properly change the  $k_{eff}(\text{code})$  to the correct value. However, if  $k_{eff} - 1$  is appreciable, an error will still be present. In this case an iterative approach must be followed, using Eq. (B.13) instead.

There are various ways in which constants may be altered to transform  $\epsilon_{hom}$  into  $\epsilon_{het}$ . The one which was used in this study was to solve for a fictitious value of  $\nu, \nu'$ , in the  $\epsilon_{hom}$  expression which would make  $\epsilon_{hom} = \epsilon_{het}$ , i.e.,

$$\epsilon_{hom}(\nu') = \epsilon_{het}(\nu) , \quad (\text{D.14})$$

where  $\nu'$  is found from (B.14) and (B.2) as

$$\nu' = \frac{(\epsilon_{het} - 1) [\Sigma_T^f - \Sigma_{es}^f + 1/V^f (V_{\Sigma_{os}}^{im} \Sigma^{im} + V_{\Sigma_{os}}^{em} \Sigma^{em} + V_{\Sigma_{os}}^l \Sigma^l)] + \chi \Sigma_a^f}{c_{het} \chi \Sigma_f^f} . \quad (\text{B.15})$$

If Eq. (B.13) were used  $\nu'$  would be dependent on  $k_{eff}(\text{code})$ , since the R.H.S. would be multiplied by  $k_{eff}(\text{code})$ .

## APPENDIX C

## TABLES OF RESULTS

1. Conversion Ratio and Burnup

Table C.1. Conversion Ratio

Lattice Pitch (in.)	Enrichment (%)			
	1	2	3	5
9.0 (S)		0.676	0.635	0.570
10.8 (S)	0.680	0.632	0.592	0.530
13.0 (S)	0.626	0.587	0.551	0.492
14.8 (S)	0.581	0.549	0.517	0.463
13.0 (L)	0.724	0.664	0.617	0.544
14.8 (L)	0.690	0.637	0.592	0.521

Table C.2. Burnup, Mwd/MT U  
(Cycle time in days)

Lattice Pitch (in.)	Enrichment (%)			
	1	2	3	5
9.0 (S)		20,854 (1068)	33,543 (1718)	52,984 (2713)
10.8 (S)	9,296 (476)	27,632 (1415)	41,589 (2130)	64,515 (3303)
13.0 (S)	9,740 (499)	27,285 (1397)	41,083 (2104)	64,198 (3288)
14.8 (S)	8,500 (435)	25,716 (1316)	39,247 (2009)	62,237 (3185)
13.0 (L)	10,163 (1228)	27,840 (3364)	40,740 (4923)	60,894 (7357)
14.8 (L)	11,749 (1420)	29,410 (3554)	42,754 (5167)	64,500 (7794)

Table C.3. FIFA, Fissions Per Initial Fissionable Atom

Lattice Pitch (in.)	Enrichment (%)			
	1	2	3	5
9.0 (S)		1.104	1.183	1.122
10.8 (S)	0.985	1.462	1.467	1.366
13.0 (S)	1.030	1.444	1.449	1.359
14.8 (S)	0.902	1.361	1.385	1.317
13.0 (L)	1.076	1.474	1.438	1.289
14.8 (L)	1.244	1.556	1.508	1.365

2. Specific Power, Throughput and Component Fuel-Cycle Costs

Table C.4. Specific Power at Equilibrium (kw/g fissile)

Lattice Pitch (in.)	Enrichment (%)			
	1	2	3	5
9.0 (S)		1.358	1.022	0.679
10.8 (S)	2.539	1.903	1.529	1.089
13.0 (S)	2.767	2.229	1.871	1.417
14.8 (S)	2.732	2.293	1.972	1.547
13.0 (L)	1.055	0.746	0.577	0.390
14.8 (L)	1.188	0.897	0.721	0.511

Table C.5. Fabrication Plant Throughput  
(MT U/year)

Lattice Pitch (in.)	Enrichment (%)			
	1	2	3	5
9.0 (S)		527.0	327.5	207.4
10.8 (S)	1180.0	396.8	263.7	170.0
13.0 (S)	1127.7	402.5	267.3	165.3
14.8 (S)	1291.6	427.0	279.8	176.5
13.0 (L)	1081.0	394.6	269.4	180.4
14.8 (L)	933.0	373.2	256.5	170.2

Table C.6. Feed Costs  
[mills/kwhr(electrical)]

Lattice Pitch (in.)	Enrichment (%)			
	1	2	3	5
9.0 (S)		0.735	0.793	0.946
10.8 (S)	0.536	0.555	0.639	0.777
13.0 (S)	0.514	0.561	0.647	0.781
14.8 (S)	0.585	0.596	0.678	0.805
13.0 (L)	0.491	0.550	0.653	0.823
14.8 (L)	0.425	0.521	0.622	0.777

Table C.7. Core Inventory Charges  
[mills/kwhr(electrical)]

Lattice Pitch (in.)	Enrichment (%)			
	1	2	3	5
9.0 (S)		0.153	0.234	0.413
10.8 (S)	0.051	0.088	0.128	0.219
13.0 (S)	0.043	0.066	0.092	0.149
14.8 (S)	0.044	0.063	0.085	0.130
13.0 (L)	0.125	0.235	0.359	0.652
14.8 (L)	0.099	0.171	0.253	0.445

Table C.8. Fabrication and Reprocessing  
Inventory Charges  
[mills/kwhr(electrical)]

Lattice Pitch (in.)	Enrichment (%)			
	1	2	3	5
9.0 (S)		0.039	0.040	0.046
10.8 (S)	0.029	0.026	0.028	0.034
13.0 (S)	0.026	0.025	0.029	0.033
14.8 (S)	0.030	0.026	0.029	0.034
13.0 (L)	0.028	0.027	0.030	0.036
14.8 (L)	0.022	0.024	0.028	0.033

Table C.9. Fabrication Costs  
(Including Interest)  
[mills/kwhr(electrical)]

Lattice Pitch (in.)	Enrichment (%)			
	1	2	3	5
9.0 (S)		0.701	0.549	0.453
10.8 (S)	1.083	0.603	0.503	0.425
13.0 (S)	1.056	0.610	0.508	0.413
14.8 (S)	1.146	0.631	0.511	0.433
13.0 (L)	0.603	0.400	0.371	0.360
14.8 (L)	0.561	0.397	0.369	0.360

Table C.10. Reprocessing Costs  
(Including Interest)  
[mills/kwhr(electrical)]

Lattice Pitch (in.)	Enrichment (%)			
	1	2	3	5
9.0 (S)		0.150	0.122	0.096
10.8 (S)	0.191	0.134	0.111	0.084
13.0 (S)	0.186	0.132	0.111	0.085
14.8 (S)	0.191	0.138	0.114	0.086
13.0 (L)	0.168	0.099	0.072	0.043
14.8 (L)	0.158	0.095	0.068	0.039

Table C.11. Fuel Shipping Costs  
(Including Interest)  
[mills/kwhr(electrical)]

Lattice Pitch (in.)	Enrichment (%)			
	1	2	3	5
9.0 (S)		0.042	0.028	0.016
10.8 (S)	0.137	0.042	0.026	0.015
13.0 (S)	0.164	0.053	0.032	0.018
14.8 (S)	0.227	0.067	0.040	0.022
13.0 (L)	0.134	0.038	0.021	0.011
14.8 (L)	0.136	0.041	0.023	0.012

Table C.12. Storage Charges for Spent Fuel  
[mills/kwhr(electrical)]

Lattice Pitch (in.)	Enrichment (%)			
	1	2	3	5
9.0 (S)		0.012	0.008	0.005
10.8 (S)	0.028	0.009	0.006	0.004
13.0 (S)	0.026	0.009	0.006	0.004
14.8 (S)	0.030	0.010	0.006	0.004
13.0 (L)	0.025	0.009	0.006	0.004
14.8 (L)	0.022	0.009	0.006	0.004

Table C.13. Spent-Fuel Plutonium and  
Uranium Credit

[mills/kwhr(electrical)]

Lattice Pitch (in.)	Enrichment (%)			
	1	2	3	5
9.0 (S)		0.275	0.221	0.210
10.8 (S)	0.244	0.100	0.076	0.057
13.0 (S)	0.178	0.076	0.054	0.039
14.8 (S)	0.190	0.070	0.049	0.033
13.0 (L)	0.257	0.123	0.097	0.085
14.8 (L)	0.176	0.089	0.067	0.051

Table C.14. Total Fuel-Cycle Cost (Spent-Fuel Re-  
processed for Credit

[mills/kwhr(electrical)]

Lattice Pitch (in.)	Enrichment (%)			
	1	2	3	5
9.0 (S)		1.545	1.545	1.760
10.8 (S)	1.783	1.348	1.359	1.497
13.0 (S)	1.811	1.371	1.365	1.440
14.8 (S)	2.033	1.451	1.408	1.477
13.0 (L)	1.292	1.226	1.409	1.840
14.8 (L)	1.225	1.160	1.296	1.615

Table C.15. Total Fuel-Cycle Cost ("Throwaway,"  
Spent Fuel Stored)  
[mills/kwhr(electrical)]

Lattice Pitch (in.)	Enrichment (%)			
	1	2	3	5
9.0 (S)		1.682	1.652	1.879
10.8 (S)	1.864	1.323	1.330	1.474
13.0 (S)	1.829	1.324	1.314	1.398
14.8 (S)	2.062	1.393	1.349	1.428
13.0 (L)	1.406	1.259	1.440	1.886
14.8 (L)	1.265	1.163	1.301	1.631

Internal Distribution

- |                       |  |
|-----------------------|--|
| 1. W. P. Barthold     | 30. F. H. Neill                        |
| 2. S. E. Beall        | 31. E. A. Nephew                       |
| 3. M. Bender          | 32. P. Patriarca                       |
| 4. L. L. Bennett      | 33. A. M. Perry                        |
| 5. R. B. Briggs       | 34. P. H. Pitkanen                     |
| 6. R. S. Carlsmith    | 35-39. C. M. Podeweltz                 |
| 7. J. H. Coobs        | 40. B. E. Prince                       |
| 8. W. B. Cottrell     | 41. J. T. Roberts                      |
| 9. R. D. Cheverton    | 42. M. W. Rosenthal                    |
| 10. C. W. Craven, Jr. | 43. A. W. Savolainen                   |
| 11. F. L. Culler      | 44. O. Sisman                          |
| 12. J. G. Delene      | 45. M. J. Skinner                      |
| 13. G. E. Edison      | 46. O. L. Smith                        |
| 14. D. E. Ferguson    | 47. I. Spiewak                         |
| 15. T. B. Fowler      | 48. W. E. Thomas                       |
| 16. A. P. Fraas       | 49. M. L. Tobias                       |
| 17. E. H. Gift        | 50. D. B. Trauger                      |
| 18. W. O. Harms       | 51. M. E. Tsagaris                     |
| 19. P. N. Haubenreich | 52. D. R. Vondy                        |
| 20. L. Jung           | 53. G. M. Watson                       |
| 21. P. R. Kasten      | 54. F. G. Welfare                      |
| 22. H. T. Kerr        | 55. G. D. Whitman                      |
| 23. J. L. Lucius      | 56. J. V. Wilson                       |
| 24. M. I. Lundin      | 57-58. Central Research Library        |
| 25. R. N. Lyon        | 59-60. Y-12 Document Reference Section |
| 26. H. G. MacPherson  | 61-63. Laboratory Records Department   |
| 27. J. H. Marable     | 64. Laboratory Records Department,     |
| 28. H. C. McCurdy     | LRD-RC                                 |
| 29. A. J. Miller      |  |

External Distribution

- 65. R. H. Ball, AEC-SR, P. O. Box 2325, San Diego, California
- 66. D. B. Coburn, General Atomic, P. O. Box 608, San Diego, Calif.
- 67. D. F. Cope, RDT-OSR, AEC, Oak Ridge, Tenn.
- 68. E. Creutz, General Atomic, P. O. Box 608, San Diego, Calif.
- 69-71. R. B. Duffield, General Atomic, P. O. Box 608, San Diego, Calif.
- 72. A. J. Goodjohn, General Atomic, P. O. Box 608, San Diego, Calif.
- 73. S. Jaye, General Atomic, P. O. Box 608, San Diego, Calif.
- 74. R. F. Kirkpatrick, RDT, AEC, Washington, D. C.
- 75. R. E. Pahler, RDT, AEC, Washington, D. C.
- 76-90. Division of Technical Information Extension (DTIE)
- 91. Research and Development Division, ORO
- 92-93. Reactor Division, ORO